Quantifying the $\delta^{15}N$ trophic offset in a cold-water scleractinian coral (CWC): implications for the CWC diet and coral $\delta^{15}N$ as the marine N cycle proxy

Josie L. Mottram[1], Anne M. Gothmann[2], Maria G. Prokopenko[3], Austin Cordova[3], Veronica Rollinson[1], Katie Dobkowski[4], Julie Granger[1]

[1]Department of Marine Sciences, University of Connecticut, Storrs, CT, 06340, USA
[2]Departments of Physics and Environmental Studies, St. Olaf College, Northfield, MN, 55057, USA
[3]Department of Geology, Pomona College, Claremont, CA, 91711, USA
[4]Department of Environmental Studies, Woodbury University, Burbank, CA, 91504, USA

Correspondence to: Anne M. Gothmann (gothma1@stolaf.edu)

Abstract. The nitrogen (N) isotope composition ($\delta^{15}N$) of cold-water corals is a promising proxy for reconstructing past ocean N cycling, as a strong correlation was found between the $\delta^{15}N$ of the organic nitrogen preserved in coral skeletons and the $\delta^{15}N$ of particulate organic matter exported from the surface ocean. However, a large offset of 8-9 ‰ between the $\delta^{15}N$ recorded by the coral and that of exported particulate organic matter remains unexplained. The 8-9 ‰ offset may signal a higher trophic level of coral dietary sources, an unusually large trophic isotope effect or a biosynthetic $\delta^{15}N$ offset between the coral's soft tissue and skeletal organic matter, or some combinations of these factors. To understand the origin of the offset and further validate the proxy, we investigated the trophic ecology of the asymbiotic scleractinian cold water coral *Balanophyllia elegans,* both in a laboratory setting and in its natural habitat. A long-term incubation experiment of *B. elegans* fed on an isotopically controlled diet yielded a canonical trophic isotope effect of 3.0 ± 0.1‰ between coral soft tissue and the *Artemia* prey. The trophic isotope effect was not detectably influenced by sustained food limitation. A long N turnover of coral soft tissue, expressed as an e-folding time, of 291 ± 15 days in the well-fed incubations indicates that coral skeleton $\delta^{15}N$ is not likely to track subannual (e.g. seasonal) variability of diet $\delta^{15}N$. Specimens of *B. elegans* from the subtidal zone near San Juan Channel (WA, USA) revealed a modest difference between soft tissue and skeletal $\delta^{15}N$ of 1.2 ± 0.6 ‰. The $\delta^{15}N$ of the coral soft tissue was 12.0 ± 0.6 ‰, which was ~6 ‰ higher than that of suspended organic material that was comprised dominantly of phytoplankton – suggesting that phytoplankton is not the primary component of *B. elegans'* diet. An analysis of size-fractionated net tow material suggests that *B. elegans* fed predominantly on a size class of zooplankton ≥ 500 µm, implicating a two-level trophic transfer between phytoplankton material and coral tissue. These results point to a feeding strategy that may result in an influence of regional food web structure on the cold-water coral $\delta^{15}N$. This factor should be taken into consideration when applying the proxy to paleoceanographic studies of ocean N cycling.

1 Introduction

Interactions between ocean circulation and nutrient cycling modulate the marine biological carbon pump, the consequent partitioning of CO_2 between atmosphere and ocean, and thus influence planetary climate on centennial to millennial time scales (Sigman and Boyle 2000). The marine nitrogen (N) cycle is highly sensitive to these interactions, such that knowledge of modern and ancient ocean N cycling can help illuminate drivers of past climate and contextualize modern global change (*e.g.*, Altabet et al., 1994; Francois et al., 1997; Robinson and Sigman 2008; Sigman et al., 1999; Kast et al. 2019).

The main tool to investigate the oceanic N cycle history is the nitrogen (N) isotope composition (*i.e.*, the $^{15}N/^{14}N$ ratio) of particulate organic nitrogen (PON) exported from the euphotic zone and preserved in various paleo-archives, including bulk sedimentary N in anoxic sediments (*reviewed by* Robinson et al. 2023). Hereafter, we express the $^{15}N/^{14}N$ ratio in delta notation, where $\delta^{15}N$ (‰ *vs.* air) = $[[(^{15}N/^{14}N_{sample})/(^{15}N/^{14}N_{air})] - 1]*1000$. The $\delta^{15}N$-PON recorded in paleo-oceanographic archives reflects both regional N cycling processes and the balance of global ocean N source and sink terms (Sigman and Fripiat 2019; Brandes and Devol 2002). In regions of the ocean where nitrate is quantitatively consumed, the annually integrated $\delta^{15}N$-PON exported from the surface reflects the isotopic composition of thermocline nitrate (Altabet et al. 1991). The latter is influenced by the circulation history of nitrate (*e.g.*, Marconi et al., 2015), by regional N_2 fixation (*e.g.*, Casciotti et al. 2008; Knapp et al. 2008) and by water column denitrification (*e.g.,* Pride et al., 1999; De Pol-Holz et al., 2007). In regions with incomplete consumption of surface nitrate, such as Southern Ocean, the isotopic discrimination imparted during nitrate assimilation is reflected in the $\delta^{15}N$-PON, which can be used to reconstruct the degree of surface nitrate consumption in the past (*e.g.,* Sigman et al., 1999; Francois et al. 1997).

Accurate interpretation of the N cycle's paleo-history relies on the presumption that the $\delta^{15}N$-PON preserved in various palaeoceanographic archives is impervious to organic matter diagenesis. Bulk sedimentary $\delta^{15}N$ measurements are thus generally inadequate in this respect, subject to post-depositional processes (Robinson et al. 2012) – barring fast-accumulating organic-rich anoxic sediments with negligible contribution from terrestrial sources (*e.g.*, Altabet et al., 2002; Ganeshram and Pedersen, 1998). To circumvent this limitation, several "biological" archives of the $\delta^{15}N$-PON have been developed that are deemed resistant to diagenetic alteration. These include the organic matter in in diatom frustules and foraminifera tests (*e.g.*, Ren et al., 2009; Robinson and Sigman, 2008) and the organic matter in proteinaceous corals (*e.g.*, Sherwood et al. 2009; Williams and Grottoli 2010). Recently, the $\delta^{15}N$ of organic N enclosed within the aragonite mineral lattice of asymbiotic scleractinian (stony) cold-water corals (CWCs) has been found to reflect the $\delta^{15}N$-PON exported from the surface

ocean (Wang et al., 2014), offering an exciting new archive of marine N cycling (Wang et al. 2017; Li et al., 2020, Studer et al., 2018; Chen et al. 2023). A robust cold-water coral archive of δ^{15}N-PON can complement the existing suite of nitrogen proxies by reducing the potential biases inevitable for almost any individual proxy, allowing for a broader geographic and temporal reconstruction, and increasing resolution of the proxy record. Foremost, as with foraminifera and diatom shells, organic material trapped within the coral's original aragonite mineral lattice is largely protected from diagenetic alteration (Drake et al. 2021), and compromised areas can be avoided by inspecting the skeletons for contamination and recrystallization (*e.g.*, borings) using microscopic techniques (Gothmann et al. 2015). CWCs have a broad geographic distribution, being present in all ocean basins from the surface to 5000 m (Freiwald, 2002). CWCs also offer the potential to generate high-resolution records extending relatively far back in time, and corals have continuous skeletal accretion that records ocean conditions at the time of growth, so the analysis of multiple individuals provides enhanced temporal resolution of long-time record (Robinson et al., 2014; Hines et al. 2015). Unlike sediments containing microfossils (e.g. diatoms and foraminifera) CWC skeletons are not subject to bioturbation and absolute ages of this paleoarchive can be determined with decadal precision on the time scales of glacial-interglacial climate variability through U-Th series dating (Cheng et al., 2000; Goodfriend et al. 1992, Robinson et al., 2014, Li et al., 2020). Remarkably, individual coral samples can archive multiple seawater properties, such that a single CWC specimen can potentially be used to reconstruct deep (*e.g.*, Δ^{14}C, pH, temperature, and circulation proxies such as Ba/Ca and εNd) and surface ocean conditions (δ^{15}N) at a precisely-known time (U-Th dating), making CWC unique as a paleoceanographic archive (Robinson et al., 2014; Thiagarajan et al., 2014; Rae et al. 2018).

Yet an outstanding concern about the fidelity of the δ^{15}N of coral-bound organic N is a reported 8 - 9 ‰ offset between coral-bound δ^{15}N and the corresponding δ^{15}N-PON exported to regions of coral growth (Wang et al. 2014). The magnitude of this offset substantially exceeds the 3 - 3.5 ‰ expected for a single trophic transfer (Minagawa and Wada 1984), assuming CWC feed predominantly on algal material exported from the surface ocean. Wang et al. (2014) explained the magnitude of the offset by arguing that CWCs feed on the more abundant pool of surface-derived suspended organic material (SPOM), as the δ^{15}N SPOM at depth is typically ~4-5‰ higher than that of sinking PON (Altabet 1988, Saino and Hattori, 1987). While CWCs are considered generalists with regard to diet (e.g., Mortensen, 2001; Freiwald, 2002; Carlier et al., 2009; Maier et al. 2023), a number of studies suggest that many species of CWC subsist predominantly on metazoan zooplankton prey (e.g., Naumann et al. 2011; Kiriakoulakis et al. 2005; Purser et al. 2010; Tsounis et al. 2010). A zooplankton diet should result in an approximate two-level or more trophic transfer between surface PON and coral tissue (*e.g.*,

Sherwood et al. 2008), closer to the observed 8-9 ‰ offset, potentially rendering coral-bound $\delta^{15}N$ sensitive to spatial and temporal differences in trophic-level food web structure. An alternative explanation for the offset is that there is a large biosynthetic offset between the $\delta^{15}N$ of the CWC polyp and its skeletal tissue (Horn et al. 2011; Muscatine et al. 2005), assuming that CWCs' diet derives directly from sinking algal material from the surface ocean. Otherwise, there could be an atypically large N isotope fractionation associated with the trophic-level transfer between the coral diet and its tissue (>3-3.5‰), possibly borne out of intermittent starvation periods (Doi et al., 2017), which is then passed on to the organic matrix within the coral skeleton. The gap in our understanding of how corals record the $\delta^{15}N$-PON exported form the surface ocean raises questions regarding the consistency of the offset in space and time, and whether it is likely to differ among CWC species or due to intra-specific variations in diet.

Due to the challenges of accessing deep-ocean environments, the trophic ecology of cold-water corals is sparsely documented, yet is fundamental to understanding the role of CWCs in cold-water reef ecosystems and to defining their utility as paleoceanographic archives of N cycling. The nature of the $\delta^{15}N$ offset between CWC skeletal material and exported PON must be explained in order to further validate and potentially improve the use of $\delta^{15}N$ of CWC skeletons as a proxy to reconstruct the history of exported PON and to further understand the role of CWCs in benthic ecosystems. To this end, we studied *Balanophyllia elegans,* an asymbiotic scleractinian cold-water coral found along the west coast of North America that grows as individual polyps (Fadlallah, 1983). We investigated the following questions: a) Is there a large offset in $\delta^{15}N$ between coral polyp tissue and coral skeletal tissue? b) Is there an unusually large trophic-level offset between coral tissue and coral diet? c) Does *B. elegans* feed predominantly on suspended particulate organic matter (SPOM) *in situ*? or d) does *B. elegans* feed predominantly on metazoan zooplankton, resulting in a two-level trophic transfer between coral tissue and N of export? To evaluate question (a), we measured the $\delta^{15}N$ of tissue-skeleton pairs of coral samples collected in their natural habitat. To evaluate question (b), we cultured *B. elegans* corals in the laboratory in experiments where both the isotopic composition of food and the frequency of feeding was controlled. To evaluate questions (c) and (d), we also investigated the $\delta^{15}N$ of various components of the food web at a field site where *B. elegans* are found plentifully. Our observations offer novel insights on the growth and trophic ecology of *B. elegans*, providing unique new data on the N metabolism of CWC and their feeding ecology. We contextualize our conclusions to inform the use of CWC archives as a paleo-proxy for marine N cycling and ocean biogeochemistry.

2. Methods

2.1 Collection of live coral specimens

Individual specimens of the cold-water coral *Balanophyllia elegans* were collected during four sampling campaigns in March and June 2019, and September and November 2020 from the San Juan Channel near the University of Washington's Friday Harbor Laboratory off the coast of Washington State in the Salish Sea (48.5º N, -123.0º W; Figure 1). *B. elegans* is a solitary, asymbiotic cold-water cup coral native to the Pacific Northwest that can be found both in shallow rocky environments and at depths as great as 500 m (Durham and Barnard 1952). The genus *Balanophyllia* is cosmopolitan and fossil samples as old as Eocene in age have been used for paleoenvironmental study (Muhs et al. 1994; Gothmann et al., 2015; Gagnon et al. 2021). *B. elegans's* presence at near surface depths makes it an easy target for culture experiments, and *Balanophyllia sp.* can be found co-occurring with the similar but more widely applied cold-water coral archive, *Desmophyllum dianthus* (Margolin et al. 2014). Therefore, we consider the asymbiotic *Balanophyllia sp.* to be generally representative of other deep cold-water coral species.

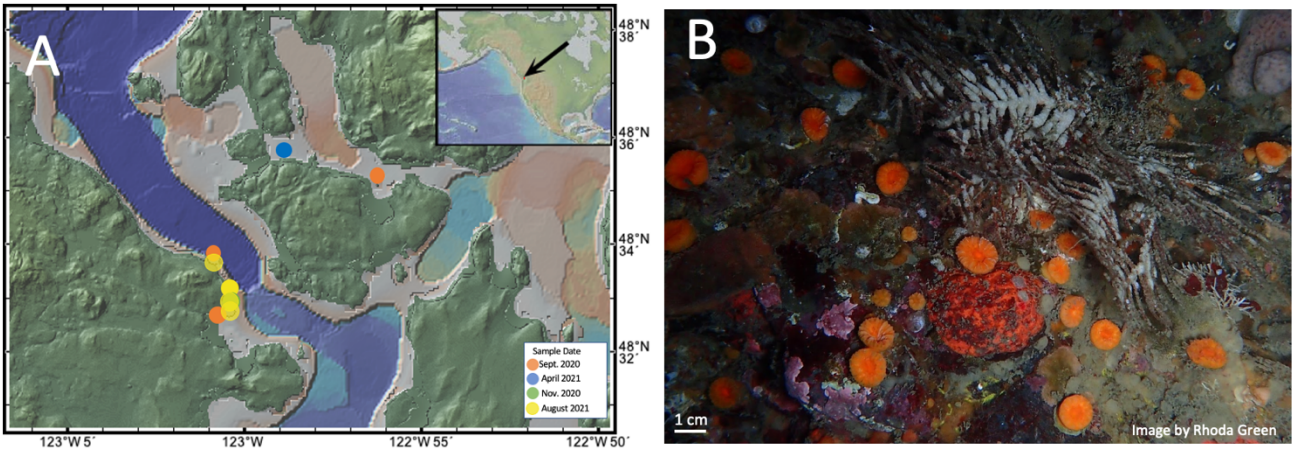

Figure 1. (a) Map of the San Juan Islands indicating the collection site of *B. elegans* specimens and hydrographic measurements (created using http://www.geomapapp.org, Ryan et al. 2009). Inset shows where the San Juan Islands are situated within North America. (b) Image of *B. elegans* from the San Juan Channel near Friday Harbor Labs taken by Rhoda Green.

B. elegans specimens were collected at 10 to 20 m depth by divers who gently removed the corals from vertical rock walls using blunt-tipped diving knives. Of the live corals collected, a subset was immediately frozen at -18ºC for N isotope ratio analyses of soft tissue and organic matter bound in the coral skeleton matrix. Live specimens were shipped overnight in small bags of seawater on ice to St. Olaf College (Minnesota, USA). Corals

were cleaned by gently scraping the exposed skeleton with dental tools to remove encrusting organisms and placed in incubation bottles with artificial seawater for recovery prior to feeding experiments (described below).

2.2 Live coral maintenance

Live *B. elegans* corals were maintained in artificial seawater medium prepared from nitrate-free Instant Ocean® Sea Salt. Salts were dissolved in deionized water to a salinity of 28.0 ± 0.25 – akin to the conditions at the collection site (Murray et al., 2015) – and sparged with air to achieve atmospheric equilibrium. The pH of the seawater was measured with a YSI brand 4130 pH probe and adjusted using dilute (0.1 N) hydrochloric acid or sodium hydroxide to 8.14 ± 0.05, slightly higher than *in-situ* conditions to promote skeletal growth. Batch seawater was then allotted to 2 L airtight polypropylene bottles to incubate single coral polyps. Bottles were pre-cleaned with fragrance-free soap and multiple rinses of deionized water. The salinity, pH, and temperature in the incubation bottles were monitored using YSI brand probes (4310(W) conductivity cell and pH probe, respectively) as well as dissolved oxygen concentrations using an optical sensor (FDO 4410; Figure S1); a Multilab 4010-3w was used as the digital meter for the sensors. The bottles containing individual corals were randomly distributed among three recirculating water baths maintained at a constant temperature of 12.5 ± 0.2 ºC, akin to the conditions at the collection site (Murray et al., 2015). Small but quasi-systematic differences of ± 0.3˚C were observed among the three recirculating tanks (Figure S2). Corals were sustained on a diet of *Artemia salina* nauplii (described below), fed twice a week to ensure maximum growth (Crook et al., 2013). Seawater in the incubation bottles was replaced twice a week after the corals were fed, based on observations indicating that seawater pH in the bottles decreased slightly but significantly by ~0.03 pH units over three days due to coral respiration (statistical analysis was performed with RStudio; Welch two sample t-test; $t(515.07)= 12.8$; p-value < 0.01; Figure S3). Dissolved oxygen concentrations remained near atmospheric equilibrium at concentration of 7.5 ± 0.3 mg L^{-1} (Figure S1). Nitrate concentrations in the bottles were also monitored from samples taken during each water change, in the freshly prepared seawater and in spent seawater, revealing low variability in NO_3^- concentration of 0.7 ± 0.3 µmol L^{-1} (Figure S4). Nitrate concentrations in the incubations were notably lower than ambient levels at the collection site, where concentration were ~25 µmol L^{-1}, ensuring that the coral's only source of nitrogen was the *Artemia* diet (Murray et al., 2015).

2.3 Coral culture experiments

2.3.1 Experiment to quantify the trophic isotope effect

The corals were acclimated to precise incubation conditions for approximately 20 hours before initiating feeding experiments. To assess the $\delta^{15}N$ of coral soft tissue compared to that of its food source, four experimental groups of individual *B. elegans* corals were fed respective diets of *Artemia salina* nauplii with different $\delta^{15}N$ values, twice per week for 530 days (Spero et al., 1993). Unhatched *Artemia salina* sourced from specific geographic locations have widely different $\delta^{15}N$ values, owing to the different N isotope dynamics of the environments from which they were collected, which makes these organisms useful for trophic studies (Spero et al. 1993). Eighteen coral specimens were fed *Artemia* nauplii hatched from cysts from the Great Salt Lake (Reference Code: GSL) with a $\delta^{15}N$ of 17.0 ± 0.3 ‰. Twelve corals were fed hatched nauplii from Lake Ulzhay in Russia (Reference Code: 1816) with a $\delta^{15}N$ of 13.8 ± 0.4 ‰. Twelve corals were fed hatched nauplii from Vinh Chau in Vietnam (Reference Code: 1805) with a $\delta^{15}N$ of 9.9 ± 0.3‰. Twelve corals were fed hatched nauplii from Tibet (Reference Code: 1808) with $\delta^{15}N$ of 6.3 ± 0.2‰. The GSL *Artemia* was procured from Aquatic Foods California Blackworm Co. (Great Salt Lake), whereas all other *Artemia* were obtained from the Artemia Reference Center (Ghent, Belgium). The $\delta^{15}N$ of the diet for each treatment was calculated as the mean value measured from each group of unhatched cysts and hatched nauplii (Table S2 and S3).

Fresh batches of nauplii were hatched from *Artemia* cysts at approximately monthly intervals, filtered into a concentrated suspension, stored frozen at -18ºC, and thawed immediately before feeding to the corals. Due to low hatch rates of the *Artemia* group 1808, corals in that treatment group were fed nauplii harvested from decapsulated *Artemia* cysts from day 151 (November 19, 2019) to 245 (February 22, 2020). The $\delta^{15}N$ of the hatched nauplii ranged from 6.3 ± 0.2 to 17.0 ± 0.3 ‰ (measured by EA-IRMS; Table S2). The $\delta^{15}N$ of the nauplii did not change significantly over prolonged storage of several months in the freezer (ANOVA test; $F(1) = 0.07$, p-value = 0.80; Figure S5). *Artemia* nauplii had a statistically indistinguishable molar C:N ratios among regional groups, averaging 6.0 ± 0.6 (ANOVA test; $F(3) = 0.31$; p-value = 0.82, Table S3). These results show that there was limited variability in the diet of corals due to freezer storage and hatching of multiple individual batches of *Artemia* (Table S2, S3, Figure S5).

Corals were fed their respective nauplii diets by transferring coral individuals from their incubation bottle to a small dish filled with artificial seawater with minimal exposure to air so as not to stress the corals. Each coral was fed 20 µL of thawed nauplii suspension by pipetting the food directly into their oral cavity, making it possible to visually ensure complete consumption and thus minimize variability in feeding rates. Each coral was

returned to its bottle with a fresh allotment of seawater when its mouth had remained closed for several minutes, signifying that it was finished eating (Figure 2).

After a shift in the $\delta^{15}N$ of diet, it is expected that coral tissue $\delta^{15}N$ will evolve as a function of time until the composition of tissue reaches an equilibrium in line with the new diet. In order to assess the rate (referred to here as the isotopic turnover time) at which this evolution occurs, individual corals were sacrificed at discrete intervals throughout the experiment. Corals were always sacrificed three days after feeding to ensure that no food remained in the oral cavity. The corals were removed from their bottles and rinsed with artificial seawater. The coral tissue was then separated from the skeleton using a fine stream of compressed air. The tissue and skeleton were frozen at -18ºC and stored separately until processed for isotope ratio analyses.

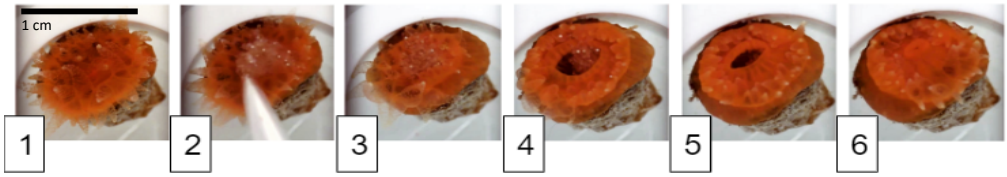

Figure 2. Photo illustration of a coral feeding sequence. Photo 1 shows coral before food is given. Photo 2 shows food being pipetted onto coral mouth. Photos 3 through 6 show the coral feeding as the mouth opens to engulf food and closes when finished, about 15 minutes in total. Corals are ~1 cm in diameter.

2.3.2 Experiment to evaluate the effects of starvation conditions

An additional 522-day feeding experiment was performed to assess the influence of starvation on the $\delta^{15}N$ of the coral soft tissue. Live corals collected during a sampling campaign at the end of November 2020 and shipped live to St. Olaf College were randomly assigned to two treatment groups (starved and not-starved). Corals in the starved treatment were fed at 25% of our normal feeding frequency, or every two weeks, whereas those in the not-starved treatment were fed twice a week. These feeding regimes were chosen based on the work of Crook et al. (2013) and Beauchamp et al. (1989), who assumed feeding every 3 days to represent plentiful food supply and feeding every 21 days (close to our starvation condition) to represent minimal maintenance food supply. Both groups were fed *Artemia* nauplii with a $\delta^{15}N$ of 9.9 ± 0.3 ‰, approximately 3 ‰ lower than the coral tissue of average *B. elegans* collected from Friday Harbor, and thus presumably closest in $\delta^{15}N$ to what the corals is eating in the wild given a canonical trophic isotope effect. Coral incubations and feedings were conducted as described above. Individuals were sacrificed over the course of the 522-day experiment, and tissue samples were frozen at -18ºC until isotope analysis.

2.4 Coral preparation for isotope ratio analyses

Frozen coral tissue samples (and hatched nauplii) were freeze-dried using a Labconco FreeZone 4.5 and then powdered using a mortar and pestle. The samples were sent to the University of Connecticut, Avery Point (Groton, CT, USA) for isotope ratio analyses.

Coral skeletons from specimens collected at Friday Harbor were separated from the coral soft tissue and were rinsed and individually and ultrasonicated two times in Milli-Q™ (MQ) water for 20 minutes each in order to remove any residual seawater. Samples were then individually ultrasonicated in a 1% sodium hypochlorite (bleach) solution for at least two 20-minute intervals with fresh bleach for each new ultrasonication interval until no tissue remained on the skeleton, as assessed visually under a dissection microscope. Individual skeletons were then rinsed and ultrasonicated for 20 minutes in MQ another three times (each time with a new batch of MQ water) in order to remove any bleach residue. Skeleton samples were sent to Pomona College (California, USA) for further processing.

It is necessary to isolate organic matter from the coral carbonate matrix in advance of the N isotope measurement methods used here (see Section 2.6 below). Organic material in the skeleton matrix was isolated and oxidized to nitrate following the protocol of Wang et al. (2014). Briefly, bulk samples weighing 50-100 mg were ground into coarse powder, and a fraction between 63 and 200 μm was collected by sieving through two metal sieves. The 10-15 mg of sieved powder was rinsed sequentially with of sodium polyphosphate-sodium bicarbonate buffered dithionite-citrate reagent, then treated with 13.5% sodium hypochlorite overnight on a shaker. Skeletal material was dissolved in 4 N ultrapure hydrochloric acid, then oxidized to nitrate by autoclaving in basic potassium persulfate solution. Standards of glutamine reference material USGS-40 and USGS-41 (respective $\delta^{15}N$ of 4.52 ‰ vs. air and 47.57 ‰ vs. air) were oxidized in tandem and used to correct for processing blanks. The resulting nitrate samples were sent to the University of Connecticut for nitrate isotope ratio analysis. The long-term averaged reagent blank was 0.4-0.6 μmol L^{-1}, while the typical samples were 10-15 μmol L^{-1} (typical amount of nitrogen in skeleton being 2-5 μmole/g of aragonite). Samples were typically run in duplicates with an average reproducibility of ~ ± 0.5 ‰. An internal laboratory standard of ground material of the cold-water colonial scleractinian coral *Lophelia pertusa* had a long-term $\delta^{15}N$ value 9.4 ± 0.8 ‰ (n=57)

2.5 Hydrographic data

To infer the natural food source of the *B. elegans*, we collected samples for analysis of the $\delta^{15}N$ of particulate and dissolved N pools in relation to ambient hydrographic variables (temperature and salinity) near Friday

Harbor, WA. Seasonal sampling campaigns were conducted in September and November 2020 and in April, June, and August 2021 (Table S1). In all but the August 2021 campaign, particulate and dissolved N samples were collected by divers at unspecified depths between the surface and the depth of coral collection. Samples were stored frozen in 30 mL HDPE bottles. Surface net tows were performed with a mesh size of 120 µm; materials were stored and shipped frozen and thawed at a later time to be filtered onto pre-combusted GF/F filters (0.7µm nominal pore size) that were stored frozen pending isotope analysis. No hydrographic variables were recorded during the campaigns except in August 2021.

During the August 2021 campaign, depth profiles of temperature and salinity from the surface to 35 m were characterized with a CastAway®-CTD (conductivity temperature depth) profiler. Water samples were collected at 5 m intervals between 5 and 30 m using a Van Dorn water sampler. Water was filtered onto pre-combusted glass fiber filters (GF/F; 0.7µm nominal pore size) into pre-cleaned 30 mL HDPE bottles and stored frozen pending analyses of nitrate concentrations and nitrate isotope ratios. The corresponding filters were stored frozen for isotope ratio analysis of suspended particulate organic material (SPOM). Surface (5 m) and deeper (25 m to the surface) net tows were conducted using plankton nets with respective mesh sizes of 150 µm and 80 µm. Net tow material was filtered directly onto a pre-combusted GF/F filters and frozen pending analysis. A portion of the net tow material from the August 2021 campaign was sieved to separate size classes of 80-100 µm, 100-250 µm, ≥ 250µm, 250-500 µm, and ≥ 500 µm. Material from the respective size classes was filtered onto pre-combusted GF/F filters and frozen until isotope analysis.

2.6 Nitrate concentrations and isotope ratio analyses

Nitrate concentrations of oxidized coral skeletons and in aqueous samples were measured by reduction to nitric oxide in hot vanadium III solution followed by chemiluminescence detection of nitric oxide (Braman and Hendrix, 1989) on a Teledyne chemiluminescence NOx analyzer Model T200 (Thousand Oaks, CA).

The $\delta^{15}N$ and $\delta^{13}C$ of lyophilized coral tissue samples were analyzed at the University of Connecticut on a Costech Elemental Analyzer–Isotope Ratio Mass Spectrometer (Delta V). Approximately 0.75 mg of lyophilized sample (35 µg N) was allotted into tin cups and analyzed in tandem with recognized glutamine reference materials USGS-40 and USGS-41 with respective $\delta^{15}N$ (*vs*. air) of 4.52 ‰ and 47.57 ‰ and $\delta^{13}C$ of -26.39 ‰ and 37.63 ‰ (*vs.* PDB). Replicate analyses of ($n \geq 2$) reference materials yielded an analytical precision of (±1 SD) of 0.3 ‰ for both $\delta^{15}N$ and $\delta^{13}C$.

Nitrate N (and O) isotope ratios of aqueous seawater samples and N isotope ratios of the skeleton matrix samples were analyzed at University of Connecticut using the denitrifier method (Casciotti et al., 2002; McIlvin and Casciotti, 2011; Sigman et al., 2001). Nitrate sample solutions were injected at target concentrations of 20 nmol for seawater samples and 7 nmol for skeleton matrix samples. N_2O was extracted, concentrated and purified using a custom-modified Thermo Gas Bench II equipped with a GC Pal autosampler and dual cold traps and analyzed on a Thermo Delta V Advantage continuous flow isotope ratio mass spectrometer (Casciotti et al., 2002; McIlvin and Casciotti, 2011). Individual analyses were referenced to injections of N_2O from a pure gas cylinder and standardized through comparison potassium nitrate reference materials International Atomic Energy Agency nitrate (IAEA-N3) and the isotopic nitrate reference material United States Geological Survey 34 (USGS-34), with respective $\delta^{15}N$ *vs.* air of 4.7 ‰ and -1.8 ‰ vs. air (International Atomic Energy Agency, 1995), and respective $\delta^{18}O$ of 25.61 ‰ and -27.9 ‰ vs. Vienna Standard Mean Ocean Water (VSMOW; Gonfiantini, 1995; Böhlke et al., 2003). To account for bacterial blanks and source linearity, nitrate concentrations of the standard material – diluted in N-free seawater for aqueous seawater samples and air-equilibrated milli-Q water for skeleton matrix samples – were matched to those of samples within batch analyses, and additional bacterial blanks were also measured (Weigand et al., 2016; Zhou et al., 2022). Replicate measurements ($n \geq 2$) of all samples yielded an average analytical precision (±1 SD) of 0.3‰ for both $\delta^{15}N$ and $\delta^{18}O$.

3. Results

3.1 Trophic isotope effect

At the onset of the culture experiment, the soft tissue among all experimental corals had a $\delta^{15}N$ of 11.7 ± 0.5 ‰. Over the course of the experiment, the $\delta^{15}N$ of the tissue increased or decreased in respective treatments depending on the $\delta^{15}N$ of their *Artemia* diet (Figure 3); the tissue $\delta^{15}N$ increased in corals fed diets with $\delta^{15}N$ values of 17.0, 13.8, and 9.9 ‰, whereas the tissue $\delta^{15}N$ decreased for the diet of 6.4 ‰. The $\delta^{15}N$ of soft tissue in all groups trended towards an asymptotic offset relative to the diet $\delta^{15}N$, as expected for an approach to a new equilibrium. However, at day 530, at the end of the experiment, it appeared as though the coral tissue $\delta^{15}N$ had not yet reached a constant offset value, suggesting that the coral tissue had not yet reached an equilibrium with the new diet. Specifically, at the end of the experiment, the coral tissue of the treatment groups reached $\delta^{15}N$ values of 9.4 ± 0.3‰, 12.6 ± 0.5‰, 15.9 ± 0.1 ‰, and 18.1 ± 0.1 ‰ for groups fed the lowest to highest *Artemia* $\delta^{15}N$ values, respectively. The difference between coral soft tissue and diet $\delta^{15}N$ ranged from a minimum of 1.0 ± 0.1‰ to a maximum of 3.0 ± 0.3‰ across the different experimental groups at day 530 (Figure 3).

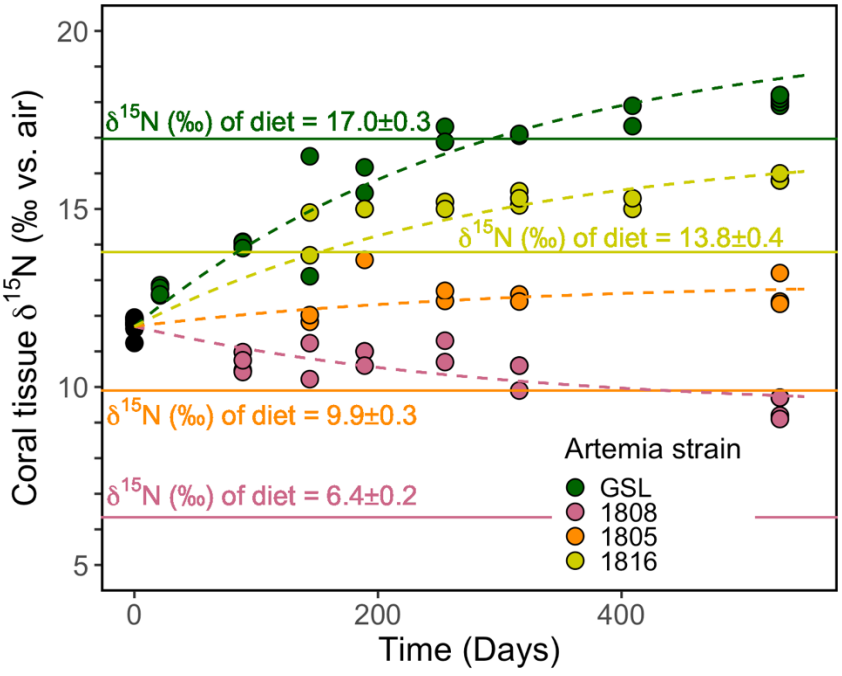

Figure 3. Evolution of the coral soft tissue $\delta^{15}N$ in response to diet $\delta^{15}N$. Colors correspond to the respective *Artemia* strains. Dashed lines are the model output of our simultaneous nonlinear least squares regression fits to the data using Equation 1. Solid lines mark the diet $\delta^{15}N \pm \sigma$. The mean analytical error on tissue $\delta^{15}N$ analyses was ± 0.2 ‰.

Despite the fact that coral tissue had not yet reached an equilibrium with the new coral diet at the end of our experiment, we are able to estimate values of the trophic $\delta^{15}N$ offset for *B. elegans*, ϵ, and the rate of isotopic turnover by fitting the data from our trophic isotope experiment to a nonlinear least-squares regression model corresponding to the isotope mixing relationship shown in Equation 1 below. Equation 1 treats the coral tissue as a single reservoir of N with some initial isotope composition that is evolving to reflect the new diet as a function of time (after Cerling et al. 2007; Ayliffe et al. 2004).

$$\delta^{15}N(t) = [\delta^{15}N_{t=0} - \delta^{15}N_{diet} + \epsilon] \cdot e^{-\lambda t} + \delta^{15}N_{diet} + \epsilon. \qquad \text{Equation 1}$$

The term $\delta^{15}N_{t=0}$ is the value of the bulk coral tissue at the onset of the experiment, $\delta^{15}N_{diet}$ is that of the corals' new *Artemia* diet (i.e. what it is fed during the experiment), t is the number of days since the start of the experiment, ϵ is the difference between the $\delta^{15}N$ of the diet and tissue at equilibrium (i.e. once the isotopic composition of inputs to the system equals the isotope composition of outputs), and λ describes the specific rate at which new N is incorporated into the coral tissue ($days^{-1}$). We use this model to calculate the e-folding time of the system, which is defined as $1/\lambda$ (days) and represents the time at which ~63% of the original N reservoir in coral tissue has been replaced with new N from the experimental coral diet.

To more confidently calculate ϵ and λ for each individual experimental group, we generate 4 equations, (one for each experimental group of the form given in Eq. 1 but with different values of $\delta^{15}N_{diet}$) and fit them simultaneously using least-squares regression. From this fit, we are able to obtain estimates for both ϵ and λ in *B. elegans*. An inherent assumption of this approach is that all experimental groups have the same e-folding time and the same trophic isotope effect. We note here that we refer to the e-folding time as the 'turnover rate' of N in corals throughout the rest of this text (e.g., Tanaka et al. 2018). Our model fit yielded a trophic isotope effect, ϵ, of 3.0 ‰ with a standard error of 0.1 ‰ between coral tissue and diet. The turnover rate of N (i.e. e-folding time, $1/\lambda$) was 291 days with a standard error of 15 days. The four individual model equations generated by our nonlinear least squares regression are presented as the dashed lines in Figure 3.

3.2 Effect of starvation

At the onset of the starvation trial, the coral tissue had an average $\delta^{15}N$ of 11.5 ± 0.1 ‰. At the end of the 522-day experiment, the starved group (N=15 coral individuals) had an average $\delta^{15}N$ of 12.4 ± 0.4 ‰ and the frequently fed group (N=15) with a $\delta^{15}N$ of 12.7 ± 0.1 ‰ (Figure 4). The starved group was +2.5 ± 0.4 ‰

compared to its diet, statistically indistinguishable from that of the frequently fed group of +2.8 ± 0.1 ‰ higher than the diet (p-value = 0.059, pairwise t-test).

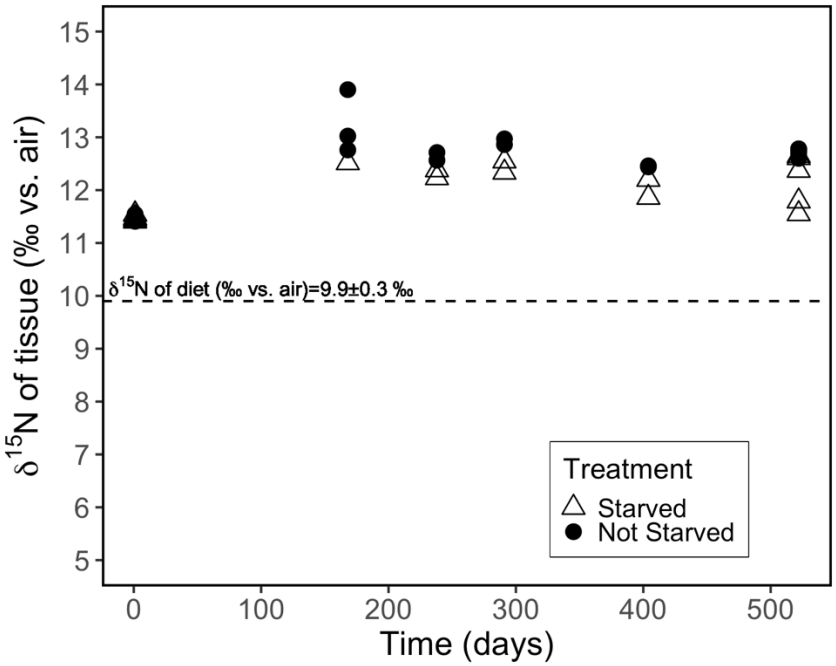

Figure 4. Evolution of the $\delta^{15}N$ of individual coral polyps fed *Artemia* nauplii ($\delta^{15}N$ 9.9 ‰) twice weekly (not starved) *vs.* every two weeks (starved). The analytical error associated with individual tissue $\delta^{15}N$ measurements was ± 0.2 ‰.

3.3 $\delta^{15}N$ comparison of field specimen polyp tissue and skeleton

The $\delta^{15}N$ of the soft tissue from individual *B. elegans* specimens collected live near Friday Harbor ranged between 11.2 to 13.1 ‰, averaging 12.0 ± 0.6 ‰ (Figure 5a). The soft tissue $\delta^{15}N$ differed among coral groups collected during different sampling campaigns, with higher values in spring (March 2019 and April 2021) compared to summer and fall (June 2019, September and November 2020; ANOVA $F(4) = 40.39$; p-value ≤ 0.01, post-hoc pairwise t-test; p-value < 0.05). The average $\delta^{15}N$ of corresponding skeletal tissue was 13.5 ± 0.7 ‰ and did not differ discernibly among sampling campaigns (ANOVA $F(2) = 0.916$; p-value = 0.431). The average

difference between skeleton and soft tissue $\delta^{15}N$ ($\Delta\delta^{15}N$) among coral individuals for which both soft tissue and skeleton was measured was 1.2 ± 0.6 ‰ (Figure 5b).

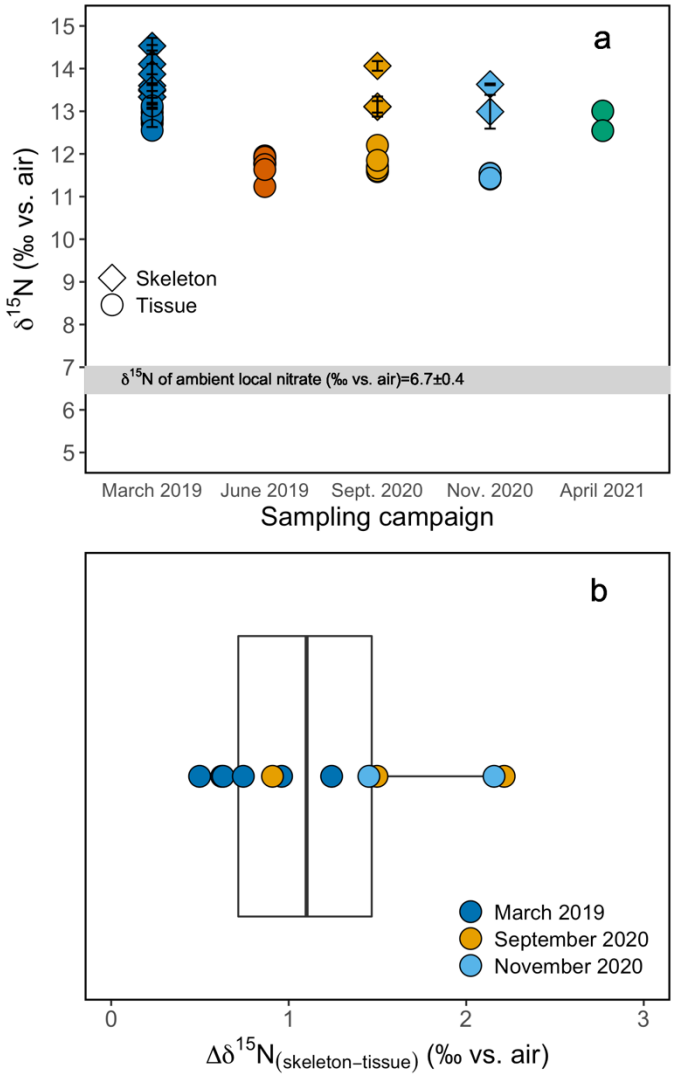

Figure 5. (a) Tissue and skeleton $\delta^{15}N$ measurements from *B. elegans* individuals collected during different sampling campaigns. Errors on skeleton data are based on replicate analyses of samples from individual polyps. (b) Boxplot of the difference between tissue and skeleton of individual *B. elegans* corals. The boxplot shows the mean, first and third quartile, maxima, and minima. Individual data points are overlaid on the plot. Colors correspond to respective sampling campaigns.

3.4 Regional hydrography and N isotope ratios of nitrate and plankton material

Hydrographic profiles recorded at stations near Friday Harbor in August 2021 showed characteristic density structures that were sensitive to tidal phase (Figure 6 a,b; Banas et al. 1999). Profiles collected during flood tide

(collected between 11:40 and 14:20 on August 2, 2021) were relatively well-mixed (salinity 30, temperature 11.8˚C), with fresher and warmer water restricted to the near surface (≤ 5 m), whereas ebb-tide profiles (collected at 9:00 on August 2, 2023) showed a progressive decrease in salinity from 30 to 27 and a corresponding increase in temperature from 11.8˚C at 35 m to 14.5˚C at the surface.

Nitrate concentrations were nearly uniform with depth during flood tide (~20 µmol L^{-1}), decreasing slightly at 5 m, whereas during ebb tide nitrate concentrations decreased progressively from 20 to 10 µmol L^{-1} between 30 and 10 m (Figure 6c). Nitrate concentrations in samples collected during the other sampling campaigns ranged from 12 to 32 µmol L^{-1}, and appeared generally higher at stations visited during the September and November 2020 campaigns compared to those in April and August 2021 (Figure S6).

Depth profiles collected in August 2021 revealed uniform nitrate $\delta^{15}N$ values of ~7 ‰ at 30 m among profiles. In well-mixed profiles, nitrate $\delta^{15}N$ increased slightly to 7.5 ‰ above 10 m. In stratified profile, nitrate $\delta^{15}N$ increased progressively to 8.2 ‰ at 10 m (Figure 6d). Among all sampling campaigns, the $\delta^{15}N$ of nitrate ranged from 6.1 ‰ to 8.2 ‰, with median values of 6.8 ± 0.4 ‰ (Figure 7a). The relationship between nitrate $\delta^{15}N$ and nitrate concentration in August 2021 was fit to a closed-system Rayleigh distillation model (Mariotti et al. 1981), suggesting a nitrate assimilation isotope effect of 1.5 ± 0.1 ‰ (Figure 8).

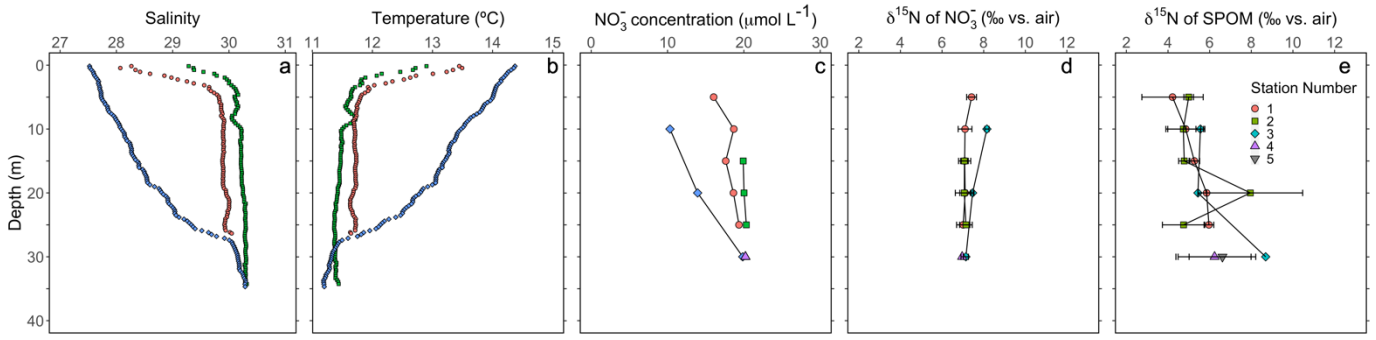

Figure 6. Depth profiles during the August 2021 sampling campaign of (a) salinity, (b) temperature, (c) nitrate concentration, (d) the $\delta^{15}N$ of nitrate for analytical replicates and (e) the $\delta^{15}N$ of SPOM of replicate samples (n ≥ 2). Green and red symbols correspond to flood tide (collected between 11:00am and 2:00pm on August 2, 2021), blue symbols correspond to ebb tide (collected at 9:00am on August 3, 2021).

The $\delta^{15}N$ of SPOM collected at depths above 35 m near Friday Harbor during the different sampling campaigns ranged from 1.6 to 11.7 ‰, averaging 5.7 ± 1.7 ‰ (Figure 7b). Values were lowest for the four samples collected in April (4.4 ± 0.4 ‰), and highest for the four samples collected in September and November (6.2 ± 2.6 ‰), although these trends may be an artifact of the low data density in April (n = 4) and Sept./Nov. (n = 5) relative to August 2021 (n = 29), at which time the observed range of $\delta^{15}N$ subsumed that in the other two

campaigns. Values did not differ coherently with depth in August 2021, although any potential depth structure was obscured by the large variability among sample replicates (Figure 6e).

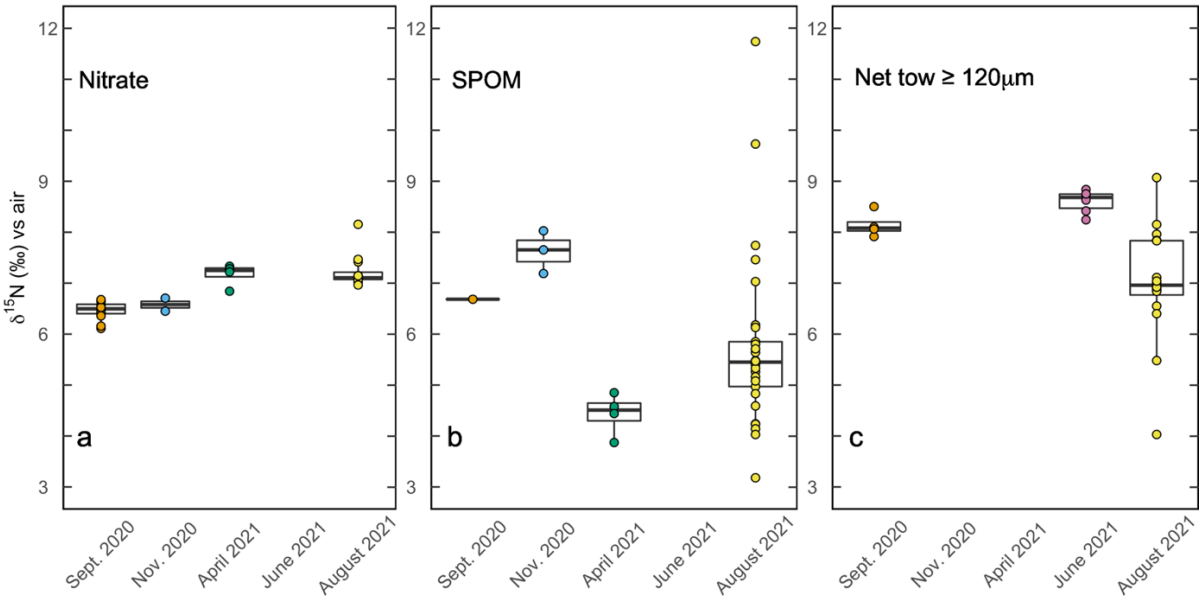

Figure 7. Boxplots of aqueous and particulate N pools at respective sampling times. (a) The $\delta^{15}N$ of nitrate from samples above 30 m collected during respective sampling campaigns. (b) The $\delta^{15}N$ of suspended particulate organic matter (SPOM) at sites near Friday Harbor during respective sampling campaigns. (c) The $\delta^{15}N$ of net tows (≥ 120 μm mesh size) conducted during respective sampling campaigns.

The $\delta^{15}N$ of material collected in net tows (120 μm mesh size) during sampling campaigns in September 2020, and June 2021 ranged between 7.9 to 8.8 ‰ (Figure 7c). Material collected in net tows of 80 μm and 150 μm mesh size in August 2021 and separated by size class post-collection revealed a coherent $\delta^{15}N$ increase with size class (Figure 7c; Figure 9). The ≥ 80 μm size class had a mean $\delta^{15}N$ of 6.0 ± 0.3 ‰ whereas that ≥ 500 μm had an average $\delta^{15}N$ of 8.0 ± 0.8 ‰, which was significantly greater than the $\delta^{15}N$ of the other size classes (ANOVA, p-value <0.05).

4. Discussion

This study of *B. elegans* provides novel constraints on the trophic ecology of scleractinian CWCs. Foremost, our observations of *B. elegans* collectively suggest that the relatively large global $\delta^{15}N$ offset of 8-9 ‰ between CWC skeletal tissue and the $\delta^{15}N$ of PON exported from the surface ocean is neither explained by a large difference between tissue and skeleton $\delta^{15}N$, nor by an unusually large trophic isotope effect. Further, controlled

feeding experiments yielded direct estimates of the trophic isotope effect and the corresponding N turnover rate of *B. elegans* soft tissue. Examination of soft tissue $\delta^{15}N$ of wild specimens in relation to regional hydrography and food web components near Friday Harbor leads us to conclude that *B. elegans* feeds predominantly metazoan zooplankton prey, implicating more than one trophic transfer between exported PON and coral soft tissue. We contextualize our findings to existing studies of CWC trophic ecology and discuss the implications of considering a two-level trophic transfer for paleo-reconstructions of ocean N cycling using *B. elegans* and CWCs more generally.

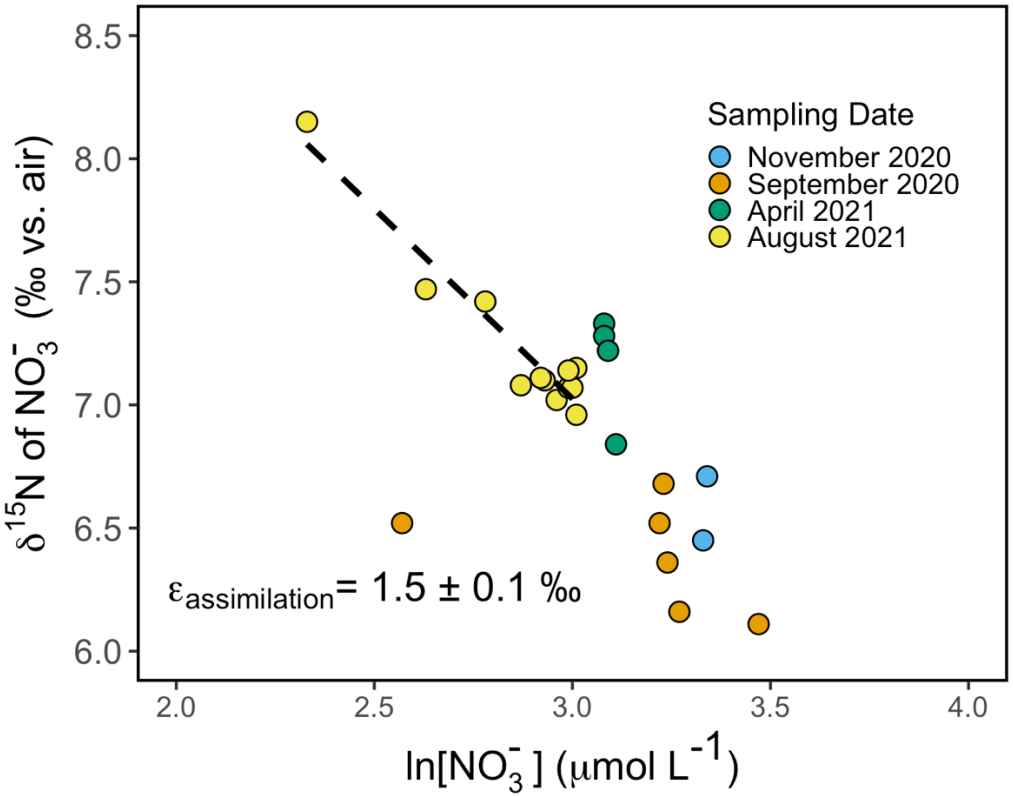

Figure 8. Rayleigh plot of nitrate $\delta^{15}N$ vs. ln of nitrate concentration for samples collected from the surface to 40 m around Friday Harbor. The isotope effect of ~1.5 ± 0.1 ‰ corresponds to the slope of the best fit linear regression line for the August 2021 data, $\delta^{15}N_{NO3} = 11.7 - 1.5 \ln [NO_3^-]$.

4.1 Culture experiments revealed a normal trophic isotope effect

We investigated whether the large difference in $\delta^{15}N$ between PON export from the surface and coral skeleton-bound $\delta^{15}N$ (8-9 ‰) observed by Wang et al. (2014) could arise from an unusually large trophic level offset specific to CWCs. The long-term feeding experiment of *B. elegans* polyps revealed a 'normal' trophic

390 isotopic offset between coral tissue and diet of ε = +3.0 ± 0.1 ‰. This value conforms to the expected range of
391 +3.4 ± 1.1 ‰ for a single trophic level offset in $\delta^{15}N$ (Minagawa and Wada, 1984).
392

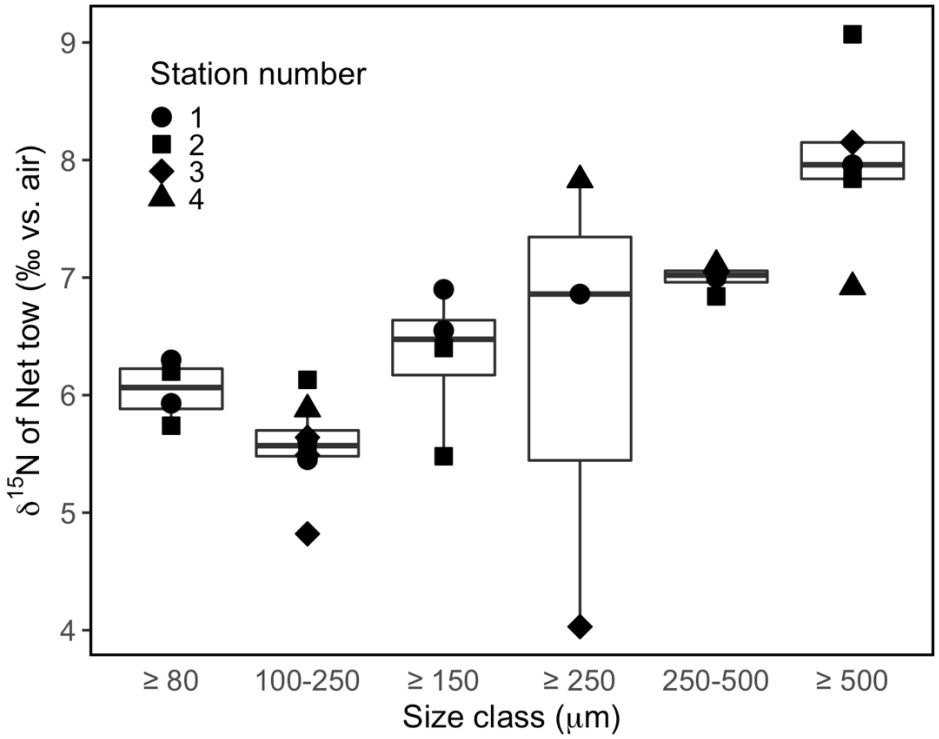

Figure 9. Boxplots of net tow material collected above 30 m in August 2021, separated by size class.

393

394 To support the above conclusion, we assess the assumptions inherent to the isotope mixing model (Eq. 1)
395 used to derive ε and the corresponding nitrogen turnover rate from our culture data. First, the model only
396 accounts for the turnover of a single pool of N, requiring the assumption that all N in the coral polyp tissues
397 equilibrate at the same rate. This notion is unlikely to be wholly accurate, as fluxes of N may vary among tissue
398 types. However, given the relatively low resolution of our sampling over the course of the culture experiments
399 (necessary due to constraints on numbers of total samples) we are unable to extend our model to one with
400 multiple pools (*e.g.* as in Ayliffe et al. 2004). As soft tissues of individual coral polyps were homogenized, we
401 suggest that the $\delta^{15}N$ values and corresponding estimate of ε thus represent the average of soft tissues with
402 potentially different turnover rates. The estimates of ε and N turnover rate further rely on the assumption that the

nutritional quality of the respective diets among treatments was equivalent, as trophic isotope effects can be sensitive to food type. Diets low in protein can be associated with greater ε values due to internal recycling of nitrogen (Adams and Sterner, 2000; Webb et al., 1998). For instance, locusts fed a low protein diet were enriched 5.1 ‰ from their diet, compared to 2.3‰ for those fed a high protein diet (Webb et al., 1998). Conversely, a compilation of studies of various metazoan consumers raised on controlled diets suggests that high protein diets generally result in higher trophic isotope effects (~3.3 ‰) compared to more herbivorous diets (~2.2 ‰), a dynamic ascribed to higher rates of N excretion to assimilation in consumers fed high protein diets (McCutchan Jr et al., 2003). As noted in Table S3 and in Section 2.3.1, our *Artemia* prey had similar C:N ratios among treatments, in line with our model treatment. Finally, our model assumes that N turnover was dominated by metabolic tissue replacement, rather than net growth, consistent with the observation that adult *B. elegans* growth is slow (Gerrodette 1981).

Equation 1 could be invalidated if the corals can access nutritional N sources other than N in *Artemia*, given that the model assumes that *Artemia* are the only source of N to corals in our experiment. Biological N_2 fixation and chemoautotrophy have been detected in association with CWC holobionts, providing some N nutrition to the corals (Middelburg et al., 2016). Our trophic isotope effect estimate was in the range expected for a single trophic transfer, arguably suggesting that N_2 fixation, if occurring, was not a substantial contribution to the corals' nutrition; it would otherwise result in a lower value of ε given a $\delta^{15}N$ contribution of -1 to 0 ‰ (Carpenter et al. 1997). That the trophic isotope effect of the poorly fed corals did not differ from that of corals that were well-fed also argues for no sources of N additional to the *Artemia*, as starved corals would presumably increase their reliance on said source. In a related vein, N recycling between the *B. elegans* specimens and potential microbial symbionts (e.g. Middelburg et al. 2016) could also dampen the trophic isotope effect relative to the *Artemia* prey and yield an over-estimate of soft tissue turnover rate for N. The normal trophic isotope effect indicated here suggests a modest role of N retention and recycling by microbial symbionts, in contrast to tropical symbiotic corals wherein bacterial symbionts promote substantial N retention and recycling, and consequently lower trophic isotope effects (Tanaka et al. 2018). Finally, the validity of our estimates could be sensitive to differences in feeding rates, which can influence the rate of N turnover of tissues (Martínez del Rio and Carleton, 2012; Rangel et al., 2019). Corals were fed at identical times among treatments, at a relatively high feeding rate (Crook et al., 2013). However, given the limited number of studies on feeding in *B. elegans*, it is difficult to compare our feeding strategy and that of this species' natural environment. Overall, we consider that the mixing model

described by Equation 1 is appropriate to derive the first-order trophic isotope effect and turnover rate of *B. elegans*.

Changes in metabolism due to underfeeding or prolonged fasting have the potential to increase trophic-level isotope offsets due to increased protein metabolism (Adams and Sterner, 2000). For instance, extensive amino acid recycling in overwintered adult insect larvae was cited to explain trophic isotope effects upward of 10‰ (Scrimgeour et al., 1995). A meta-analysis on the effects of starvation on consumer $\delta^{15}N$ revealed that starvation generally led to increased organism $\delta^{15}N$ by an average of 0.5 ‰, up to 4.3 ‰ (Doi et al., 2017). This dynamic was documented for the tropical symbiotic coral *Stylophora phistillata,* where heterotrophically starved corals were enriched in $\delta^{15}N$ by ~0.5 ‰ compared to frequently fed corals (Reynaud et al., 2009). The trophic isotope offset of *B. elegans* soft tissue relative to its diet, ε, was not discernibly influenced by near starvation; that of corals fed once every other week was similar to that of corals fed twice a week – in spite of visible signs of stress among the former, including relatively more sluggish feeding (Figure S7) and thinner soft tissue (data not shown). Deep sea coral reefs are often highly productive environments with high levels of biodiversity, commensurate with a relatively high food supply (Duineveld et al., 2007; 2004; Genin et al., 1986; Roberts et al., 2006; Soetaert et al., 2016; Thiem et al., 2006; Cathalot et al. 2015). Nevertheless, periodicity and spatial heterogeneity in the food supply of CWC reefs implicate periods of lower food density (e.g., Duineveld et al. 2007). High currents, downwelling and/or vertically migrating zooplankton temporally boost the export of surface organic matter to the seabed, creating 'feast' conditions, interspersed with 'famine' periods during the non-productive season (Maier et al. 2023). Regardless, our trials suggest that starvation, if pertinent to CWC communities, does not result in greater-than-expected trophic isotope offsets, at least for *B. elegans*.

4.2 Turnover rate for *B. elegans*

We report the first estimate of the nitrogen turnover for a non-symbiotic cold-water coral of 291 ± 15 days for *B. elegans* soft tissue. This value falls within the range of existing estimates for tropical symbiotic corals. Pulse-chase experiments with ^{15}N-nitrate conducted with fragments of the tropical symbiotic coral *Porites cylindrica* yielded a N turnover time of 370 days, and of 210 days for the tropical symbiotic coral *Acropora pulcra* (Tanaka et al. 2006; 2018). These relatively long turnover times are attributed to the recycling and retention of N within the coral-symbiont system in nutrient-deplete ecosystems. In comparison, the corresponding carbon turnover in *A. pulcra* was 18 days – compared to 210 days for N – because the system is ultimately N limited (Tanaka et al., 2006). Tanaka et al. (2018) inferred that the N turnover in *P. cylindrica* would be substantially faster than 370 days without symbionts, on the order of 56 days based on estimates of polyp-specific

N uptake rates. Nevertheless, the N turnover estimated for the tropical symbiotic coral *Porites lutea* was notably shorter that *A. pulcra and P. cylindrica*, on the order of 87 days (Rangel et al., 2019), implicating different N nutritional strategies among symbiotic coral groups and/or ecosystems. The N turnover for *B. elegans* estimated here is of the same order as but still longer than that for tropical symbiotic corals suggesting that cold-water species have lower metabolic and growth rates compared to tropical symbiotic species, although efficient N recycling has also been documented previously in cold-water corals (Middelburg et al. 2016). The slower turnover of CWCs relative to their symbiotic tropical counterparts may reflect the lower temperatures of the former's habitats (Miller, 1995; Thomas and Crowther 2015).

Constraints on N turnover also allow for calibration of the temporal resolution that is achievable with the CWCs $\delta^{15}N$ proxy for marine N cycling. Corals are constantly accreting skeleton, such that coral proxies have the potential to provide annual resolution (*e.g.*, Adkins et al. 2004). In theory, a rapid N turnover in CWC could record seasonal changes in regional N dynamics. A turnover time of 291 ± 15 days for N in *B. elegans* soft tissue, however, signifies that the $\delta^{15}N$ of coral skeleton is unlikely to provide a faithful record of seasonal differences in the $\delta^{15}N$ of the coral diet. Moreover, the turnover of the pool of N that sources the skeletal tissue may be different from that of bulk tissue, and thus decoupled from the soft tissue turnover rate. We suggest that CWCs can likely record changes in their diet on annual or longer timescales, compatible with the ability to date CWC with subdecadal resolution (Adkins et al. 2004).

4.3 Soft tissue vs. skeleton $\delta^{15}N$

A large biosynthetic $\delta^{15}N$ offset between the coral soft tissue and its skeleton could conceivably account for a large $\delta^{15}N$ offset between coral skeleton-bound organic matter and N of export that is not explained by single trophic level enrichment of ~3 ‰. However, the mean difference between soft tissue and skeleton-bound $\delta^{15}N$ among *B. elegans* specimens collected at Friday Harbor was relatively modest, on the order of +1.2 ‰, ranging between +0.5 and +2.2 ‰. The observed range was dictated primarily by the variability in the $\delta^{15}N$ of the coral soft tissue, as skeleton-associated $\delta^{15}N$ values were relatively invariant among specimens sampled from different locations and field seasons – likely due to the fact that the amount of skeleton analyzed represented multiple years of growth. The amount of skeleton-bound organic N is small relative to aragonite mass (2-5 μmol N per g of skeleton in our samples), such that homogenization of 50-100 mg aragonite fragments may alias seasonally-driven variability in skeletal $\delta^{15}N$. Soft tissue values in spring were ~1.5 ‰ higher than in summer and fall, such that they appeared to record seasonal changes in diet (Figure 5a). In this regard, the asymptotic nature of the two end-member isotope mixing model (Eq. 1) renders *B. elegans*'s soft tissue sensitive to seasonal changes in prey

492 $\delta^{15}N$, but not likely to reach isotopic equilibrium on seasonal timescales - given an N turnover of ~291 days, as
493 discussed above. Seasonal variations in the $\delta^{15}N$ of the food source of *B. elegans* near Friday Harbor could arise
494 from corresponding differences in the $\delta^{15}N$ of nitrate entrained to the surface driven by seasonal hydrographic
495 variability around San Juan archipelago, in the extent of surface nitrate consumption, in food web structure, or
496 from some combination of these. The data density among all but the August 2021 sampling campaign is too
497 sparse to be conclusive in this regard. Otherwise, the observed differences in soft tissue $\delta^{15}N$ may result from
498 spatial heterogeneity in food source $\delta^{15}N$ among the different collection sites visited for respective campaigns at
499 Friday Harbor.

500 As documented here for *B. elegans*, the $\delta^{15}N$ difference between coral tissue and skeleton appears to be
501 modest among various scleractinian coral species. Specimens of the symbiotic tropical coral *Porites lutea* showed
502 a $\delta^{15}N$ offset of +1.1 ‰ between skeleton and soft tissue, whereas the symbiotic tropical coral *Favia stelligera*
503 revealed an insignificant offset of -0.1 ‰ (Erler et al., 2015). Similarly, no offset was observed for proteinaceous
504 cold-water corals of the genus *Lepidisis* collected off Tasmania (Sherwood et al., 2009), whereas an offset of -1.9
505 ± 0.8 ‰, was reported for cold-water proteinaceous corals of the genus *Primnoa* from the Gulf of Alaska,
506 *Isadella* from the Central California Margin, and *Kulamanamana* from the North Pacific Subtropical Gyre
507 (McMahon et al., 2018). Conversely, a study of numerous species of both symbiotic and non-symbiotic corals
508 reported a +4 ‰ offset between the skeletal organic matrix and soft tissue among the non-symbiotic corals
509 specifically, but no difference among the symbiotic corals (Muscatine et al., 2005), suggesting that biosynthetic
510 offsets may occur for certain CWC species or conditions.

511 4.4 Implications for components of CWC diet

512 Cold water corals are considered opportunistic feeders, ingesting whatever is available in the water column
513 (Mortensen, 2001; Freiwald, 2002; Duineveld et al. 2004; 2007; Kiriakoulakis et al. 2005; Carlier et al. 2009;
514 Dodds et al. 2009; van Oevelen et al. 2009). They are reported to feed on zooplankton (Kiriakoulakis et al., 2005;
515 Naumann et al., 2011), including microzooplankton (Houlbrèque et al. 2004), on phytoplankton and
516 phytodetritus, including the bacterial fraction of phytodetritus (Maier et al., 2020; Houlbrèque et al. 2004),
517 dissolved organic matter (Mueller et al., 2014; Ferrier 1991, Al-Moghrabi et al. 1993; Hoegh-Guldberg &
518 Williamson 1999; Houlbrèque et al. 2004; Grover et al. 2008), and the CWC holobiont has been observed to
519 display biological N_2 fixation and chemoautotrophy (Middelburg et al. 2016). While it is clear that corals may be
520 able to consume a variety of components within the food web, the soft tissue $\delta^{15}N$ of *B. elegans* specimens
521 collected at Friday Harbor averaged 12.0 ‰, signifying that they fed on material with a $\delta^{15}N$ of approximately

9.0 ‰ – accounting for a normal trophic offset relative to their diet (3 ‰) confirmed by our culture experiment results. Here, we seek to determine the primary nutrition source for *B. elegans* at Friday Harbor by comparing the $\delta^{15}N$ of these corals' expected diet with measured $\delta^{15}N$ of different food web components including SPOM and net tow material.

We first explore whether the SPOM fraction of the food web was the dominant component of *B. elegans'* diet at Friday Harbor. SPOM is operationally defined as the particulate material retained onto glass fiber filters (GF/F, 0.7µm nominal pore size) from filtered aqueous samples. At the ocean surface, including at the stations near Friday Harbor, SPOM is generally dominated by phytoplankton material. At the ocean subsurface, below the euphotic zone, SPOM derives from organic material exiting the ocean surface, but is considered a distinct pool from the ballasted sinking PON collected in sediment traps. The $\delta^{15}N$ of SPOM typically increases with depth, with the steepest gradient across the 100-300 m depth interval, reaching upwards of ~4-5 ‰ in the ocean subsurface, which are higher values than the corresponding sinking particles at abyssal depths due to recycling and remineralization (Altabet, 1988; Casciotti et al., 2008; Saino and Hattori, 1987). Wang et al. (2014) reasoned that because the $\delta^{15}N$ of SPOM is approximately one trophic level lower that of the N preserved in skeletons of the deep-dwelling (deeper than ~ 500 m) CWC *Desmophyllum dianthus,* and because suspended particles are the most abundant form of small particles in the deep ocean, cold-water corals must feed predominantly on SPOM. However, SPOM collected in the upper 30 meters near Friday Harbor was 5.7 ± 1.7 ‰, which is ~ 6 ‰ lower than *B. elegans* soft tissue, a difference greater than expected for a single trophic level. Thus, the SPOM at Friday Harbor was evidently not the predominant food source for *B. elegans* growing in this depth interval.

Additionally, it has been suggested that CWCs can assimilate dissolved organic nitrogen (DON) (Gori et al., 2014). We do not have $\delta^{15}N$ DON measurements from our field study. However, we do not expect the potential assimilation of DON to explain the elevated $\delta^{15}N$ of organic tissue that was observed. There are two components of marine DON, refractory and labile (Bronk et al. 2002), which have different $\delta^{15}N$ (Knapp et al. 2018). At Friday Harbor, we don't know the partitioning of the $\delta^{15}N$ between these pools, but even if we did, the labile fraction (which would presumably be the pool available to corals) is expected to converge on the $\delta^{15}N$ value of SPOM (Bronk et al., 2002, Sigman and Fripiat 2019 their Fig. 4; Knapp et al., 2018, Zhang et al., 2020), given that the most recently produced DON is generally most labile. As a result, consumption of DON would not explain the high $\delta^{15}N$ of coral organic tissue.

Instead, we suggest that the relatively high $\delta^{15}N$ of ~ 12 ‰ of *B. elegans* soft tissue at Friday Harbor results from these corals deriving nutrition predominantly from larger metazoan zooplankton. Indeed, this is supported by a comparison of the $\delta^{15}N$ coral tissue and the $\delta^{15}N$ of the largest size class of net tow material (≥ 500 µm) of

8.0 ± 0.8 ‰. This is the only component of the organic matter nitrogen budget that is offset from the coral tissue by ~ 3.5 ‰, consistent with one trophic level transfer. Additionally, the net tow material had a molar C:N ratio of 4.4 ± 0.6, compared to 6.5 ± 2.2 for the SPOM (Figure S8), suggesting a dietary preference for metazoan zooplankton would provide higher protein content and nutritional density for these corals (Adams and Sterner, 2000).

Despite evidence for zooplankton as the main dietary source for *B. elegans* at Friday Harbor, we acknowledge that this feeding strategy may not apply for corals of other species living in habitats that are hundreds to thousands of meters deep. As pointed out in a recent review (Maier et al. 2023), the presence of CWC reefs in the food-limited deep ocean appears paradoxical, and it is not likely that the food available to corals at Friday Harbor looks identical to food available to corals living at >1000 m water depth. Indeed, Maier et al. 2023 suggest that the biodiversity and productivity of CWC reefs in the deep sea are supported by a number of processes such as CWC's ability to consume a range of dietary components (DOM, bacterioplankton, inorganic resources such and inorganic C and ammonium), efficient resource recycling, and their ability to align their feeding strategies and growth with fluctuations in food availability.

Maier et al. (2023) and references therein highlight that most deep CWC reefs occur in regions with higher-than-average annual primary productivity, indicating that these CWC reefs are sustained by inputs of high energy to the system, where there is also evidence for the presence of vertically migrating zooplankton. The vertically migrating zooplankton have been found near both relatively shallow (<200 m, Duineveld et al. 2007, Garcia-Herrera et al., 2022) and deep (~1000 m, e.g. Carlier et al. 2009) CWC reefs. Moreover, there are a number of other independent studies that reveal a single trophic level offset between the $\delta^{15}N$ of zooplankton prey and the $\delta^{15}N$ soft tissue of asymbiotic scleractinian corals at specific sites (Duineveld et al., 2004, Sherwood et al. 2005; 2008; 2009; Carlier et al., 2009; Hill et al., 2014; Maier et al., 2020). Given the 'normal' trophic level offset reported for CWCs in our laboratory culture experiment, these published observations underscore that zooplankton could be a dominant dietary component of corals other than *B. elegans* as well. Additional evidence from lipid biomarkers corroborates the assertion that deep-dwelling CWC species such *Lophelia pertusa* (recently re-classified as *Desmophyllum pertusum*) and *Madrepora oculata* feed predominantly on metazoan zooplankton (Dodds et al., 2009; Kiriakoulakis et al., 2005; Naumann et al. 2015). Some deep-dwelling CWCs (*Desmophylum pertusum, Madrepora oculata, Dendrophyllia cornigera*) exhibit prey preference for larger zooplankton (Da Ros et al. 2022), suggesting that zooplankton prey are an essential component of their diet. Indeed, an exclusive diet of phytodetritus (Maier et al. 2019) and the exclusion of zooplankton from diet

583 (Naumann et al. 2011) led to decreases in coral metabolism. More fundamentally, the shared traits of tentacles
584 and nematocysts are evidence of a predatory life strategy, indicating that zooplankton are an important food
585 source for corals (Lewis and Price, 1975; Sebens et al., 1996). The coral morphology of *B. elegans* and that of
586 other cold water scleractinian corals is consistent with an adaptation for the capture of prey of a commensurate
587 size (Fautin, 2009). Correspondingly, *D. dianthus* is considered to be a generalized zooplankton predator that can
588 prey on medium to large copepods and euphasiids (Höfer et al., 2018). In contrast, gorgonian corals do not
589 capture naturally occurring zooplankton and have a correspondingly low density of nematocysts (Lasker 1981).
590 In summary, while our data cannot directly indicate that all CWCs, including the deep-dwelling ones, derive their
591 primary nutrition from zooplankton, the results of our trophic experiment and field study (when evaluated in the
592 context of the published literature) suggest that it may be important to consider metazooplankton as a significant
593 component of CWC diet, and that CWC $\delta^{15}N$ is likely to be sensitive to food web dynamics. We discuss the
594 implications of these suggestions further in the sections below.

595 4.5 Does coral-bound $\delta^{15}N$ reflect surface ocean processes at Friday Harbor?

596 The effectiveness of coral skeleton-bound $\delta^{15}N$ as an archive to reconstruct past ocean N cycling depends on
597 its ability to record the $\delta^{15}N$ of the surface PON export. In turn, the $\delta^{15}N$ imparted to the phytoplankton
598 component of surface particles, from which PON export derives, is highly dependent on surface ocean dynamics
599 that influence the degree of nitrate consumption and associated isotope fractionation. Here, we describe local
600 marine N cycling dynamics in order to evaluate whether coral-bound $\delta^{15}N$ recorded in the *B. elegans* specimens
601 reflects local surface ocean processes.

602 Given complete assimilation of inorganic N pools, the $\delta^{15}N$ of phytoplankton material - the dominant
603 component of SPOM at the surface ocean - converges on the $\delta^{15}N$ of the N sources, new nitrate and recycled N
604 sources (Treibergs et al., 2014; Fawcett et al. 2011). At steady state, the $\delta^{15}N$ of the sinking PON flux reflects the
605 isotope signature of the nitrate upwelled to the surface (Altabet, 1988). Alternatively, given partial nitrate
606 consumption in the context of a finite pool (Rayleigh dynamic), such as in high-nutrient low-chlorophyll regions
607 and in upwelling systems, the SPOM $\delta^{15}N$ is fractionated relative to the nitrate $\delta^{15}N$ as function of the
608 assimilation isotope effect and the extent of nitrate consumption (Sigman et al., 1999). The $\delta^{15}N$ of the sinking
609 flux then reflects both the $\delta^{15}N$ of nitrate upwelled to the surface and the degree of nitrate consumption (Altabet
610 and François 1994; François et al. 1997). In this section, we discuss whether coral-bound $\delta^{15}N$ reflects the $\delta^{15}N$ of
611 nitrate entrained to the surface.

Nitrate assimilation at Friday Harbor appeared to be incomplete, potentially implicating the fractionation of N isotopes between nitrate and biomass. Although depleted nitrate concentrations are generally expected at coastal sites during the summer in density stratified water column due to phytoplankton assimilation, nitrate concentrations at Friday Harbor in August of 2021 were upwards of 15 μM at the surface and 20 μM at 30 m depth. Indeed, nitrate in the San Juan Channel is replete year-round, even at the surface, due to vigorous mixing within the channel (Mackas and Harrison, 1997; Murray et al., 2015).

The region experiences tidal mixing, designating it as a well-mixed estuary with minimal density stratification (Banas et al., 1999; Mackas and Harrison, 1997). The tidal influence is clearly identified from the diurnal patterns of vertical hydrographic structure variability with the salinity/temperature gradients changing with the tidal phase (Figure 6a and b). The tidal pumping drives vertical mixing between high nutrient deep water from the Juan de Fuca Strait and fresher surface water from the Strait of Georgia (Banas et al., 1999; Lewis, 1978; Murray et al., 2015; Mackas and Harrison, 1997). Nutrient concentrations in the surface Georgia Strait vary seasonally and are depleted during the summer at the stratified, fresher surface (Del Bel Belluz et al., 2021; Mackas and Harrison, 1997). Our temperature-salinity plot in August 2021 reflects end-member mixing between more saline/colder water from the Juan de Fuca Strait with fresher/warmer surface water from the Georgia Strait (Figure S9; Banas et al., 1999). The influence of Georgia Strait surface water is recognized by the salinity minima originating from the outflow of the Fraser River (Figures S10; Mackas and Harrison, 1997). The nitrate profiles in August 2021, though collected with a lower vertical resolution, do show diurnal variability in vertical gradients similar to salinity/temperature, consistent with the tidal mixing effect (Figure 6c).

The $\delta^{15}N$ of nitrate measured at stations near Friday Harbor also corroborate the mixing of nitrate-rich deeper water with nitrate-deplete surface water from Georgia Strait. The apparent isotope effect for nitrate assimilation in August 2021 was ~1.5 ‰, markedly lower than the canonical value of 5 ‰ associated with nitrate assimilation by surface ocean phytoplankton communities (DiFiore et al., 2006; Sigman et al., 1999; Altabet and François, 1994). A low apparent isotope effect is consistent with two end-member mixing of lower $\delta^{15}N$, nitrate-rich water with highly fractionated (high $\delta^{15}N$), low-nitrate water (Sigman et al., 1999). Highly fractionated nitrate, in turn, likely originated from nutrient-depleted Georgia Strait surface waters entrained into the Channel Islands. The linear relationship between salinity and nitrate concentration in August 2021 further substantiates physical mixing as the dominant control on nitrate concentrations and isotope ratios in San Juan Channel (Figure S10; Mackas and Harrison, 1997). Moreover, the $\delta^{15}N$ of nitrate was relatively uniform with depth, indicating effective vertical mixing of the Georgia Strait and Juan de Fuca Strait water masses. The relatively slight decrease in

642 nitrate $\delta^{15}N$ with depth suggests a secondary influence of local nitrate assimilation on its concentration and
643 isotope ratios.

644 The corresponding $\delta^{15}N$ of SPOM at Friday Harbor covered a broad range, from 4.2 ‰ to 8.7 ‰ in August
645 2021. The depth distribution of SPOM did not mirror the corresponding nitrate $\delta^{15}N$ profile, as could otherwise
646 be expected. At the stratified near-surface (5 m) at station 1, the $\delta^{15}N$ of SPOM averaged 4.2 ‰ compared to 7.4
647 ‰ for nitrate. In the context of Rayleigh fractionation, this result suggests that particulate material at the surface
648 consisted primarily of the instantaneous product of nitrate assimilation (Mariotti et al., 1981). The lower $\delta^{15}N$
649 SPOM values could also reflect some degree of reliance on regenerated N species, which would result in $\delta^{15}N$ of
650 SPOM lower than that of incident nitrate (Fawcett et al., 2011; Lourey et al., 2003; Treibergs et al., 2014).
651 Deeper in the water column, the $\delta^{15}N$ of SPOM converged on the $\delta^{15}N$ of incident nitrate, between 6 and 7‰,
652 suggesting that SPOM derived from the complete consumption of an incident nitrate pool (even though nitrate
653 was present at these depths). Phytoplankton at these depths may thus have originated from surface water
654 entrained from the Strait of Georgia – where nitrate was completely utilized. The above dynamics complicate
655 validation of the offset between $\delta^{15}N$ of exported PON and coral-bound $\delta^{15}N$. Yet we find little evidence for
656 nitrate fractionation from partial assimilation on $\delta^{15}N$ of phytoplankton SPOM, which suggests that the $\delta^{15}N$
657 imparted on local *B. elegans* skeletons should reflect the $\delta^{15}N$ of nitrate entrained to the surface. The ~ 7‰
658 difference between coral skeleton $\delta^{15}N$ (~13.5‰) and the entrained nitrate (~6.5‰) is similar to the empirical
659 range of 7 - 9‰ reported for other CWC species, (e.g. *D. petusa,* Kiriakoulakis et al., 2005) and *D. dianthus*
660 (Wang et al. 2014) and suggests that *B. elegans* provides a record of the thermocline nitrate $\delta^{15}N$ and surface
661 nutrient dynamics at Friday Harbor.

662 **5. Conclusions and implications for paleo-reconstruction from coral $\delta^{15}N$**

663 We conclude that the solitary scleractinian cold water coral *B. elegans* in Friday Harbor, WA predominantly
664 derives nutrition from metazoan zooplankton prey. While our study was limited to a shallow field site, our
665 isotope feeding experiment, evaluated alongside previously published studies, points to the possibility that
666 deeper-dwelling CWCs could also rely on zooplankton prey as a fundamental component of their diet. SPOM
667 may contribute to these CWCs' diet, but it cannot be presumed to exclusively account for the large offset
668 between $\delta^{15}N$ of PON export and coral skeleton $\delta^{15}N$ documented by Wang et al. (2014). The $\delta^{15}N$ of skeletal
669 material recovered from coral archives is thus likely to be sensitive to local food web dynamics; for a given $\delta^{15}N$
670 of sinking PON exiting the surface ocean, the $\delta^{15}N$ recorded by CWC may differ among individuals of the same

species feeding on different zooplankton prey, depending on availability. In fact, Wang et al. (2014) did report a "natural variability" of 1-1.5‰ within a single specimen that might have resulted from some variability of the local food web on a short time scale of few years. Some studies have documented an increase in the degree of carnivory of zooplankton with depth (Dodds et al., 2009; Vinogradov, 1962). For instance, Hannides et al. (2013) recorded a 3.5 ‰ increase in zooplankton $\delta^{15}N$ from 150 m to 1000 m in the Subtropical North Pacific, with the steepest rate of increase from 100 – 300 m. Koppelmann et al. (2009) reported a similar pattern of zooplankton $\delta^{15}N$ through the water column. These findings could explain previous reports of small but resolvable (1-2 ‰) depth-dependencies of coral $\delta^{15}N$ (Wang et al. 2014) if corals feed predominantly on zooplankton with depth-dependent degree of carnivory of zooplankton and increasing with depth $\delta^{15}N$. The $\delta^{15}N$ recorded in CWC skeletons also tends to differ among species by 1-2‰, as respective species occupy different nutritional niches (Teece et al., 2011). The relationship between CWC species represented in fossil archives to the depth structure of their zooplankton prey warrants further investigation.

Consideration of the possible dependence of coral-bound $\delta^{15}N$ on food web dynamics informs the questions that can be competently addressed by this proxy. Although we do not have direct estimates of the $\delta^{15}N$ range that can be expected from local food web variability, the scatter around the global compilation of Wang et al. (2014) for coral-bound $\delta^{15}N$ of *D. dianthus* relative to the $\delta^{15}N$ of PON suggests that this range is modest, on the order of ~1-2 ‰. Given this range, we suggest that the coral-bound $\delta^{15}N$ proxy will be most useful for reconstructing larger environmental $\delta^{15}N$ signals and where chosen coral samples belong to the same species and are collected at comparable depths as has already been successfully demonstrated by Wang et al. (2017), Studer et al. (2018) and Chen et al. (2023). If used in this way, the broad geographic and temporal coverage afforded by CWCs, the opportunity to measure multiple proxies from individual specimens and the imperviousness of coral-bound $\delta^{15}N$ to diagenetic alteration render it a valuable paleo-proxy for reconstructing marine N cycling.

Data Availability Data presented in this paper is available at: https://www.bco-dmo.org/project/893811

Author Contribution JG, AG, and MP conceptualized the research presented in this paper. JM and AG designed and carried out culture experiments. MP and AC prepared coral samples for analysis. JM and VR analyzed samples. JM, AG, JG and KD collected water samples, SPOM, and net tows. KD collected live corals for culture experiments and field studies. JM and JG prepared the manuscript with contributions from all co-authors.

Competing Interests: The authors declare that they have no conflict of interest.

Acknowledgements

We are grateful to Friday Harbor Labs for their assistance with coral collections and field sampling, especially Pema Kitaeff and Megan Dethier. We acknowledge the valued assistance of the Artemia Reference Center (specifically Gilbert Van Stappen and Christ Mahieu). Coral culture experiments would not have been sustained without the help of St. Olaf undergraduate students Rachel Raser, Joash Daniel, Qintiantian Nong, YiWynn Chan, Mansha Haque, Natasia Preys and Miranda Lenz. We are also indebted to Dr. C. Tobias and P. Ruffino for access to and assistance with the Elemental Analyzer Isotope Ratio Mass Spectrometer. This projected was funded by an NSF RUI award to A.G. (OCE-1949984), M.G.P (OCE-1949132) and J.G. (OCE-1949119).

References

Adams, T.S., Sterner, R.W. 2000. The effect of dietary nitrogen content on trophic level ^{15}N enrichment. Limnol. Oceanogr. 45, 601–607. https://doi.org/10.4319/lo.2000.45.3.0601

Adkins, J.F., Henderson, G.M., Wang, S.-L., O'Shea, S., Mokadem, F. 2004. Growth rates of the deep-sea Scleractinia *Desmophyllum cristagalli* and *Enallopsammia rostrata*. Earth and Planetary Science Letters 227, 481-490. https://doi.org/10.1016/j.epsl.2004.08.022

Al-Moghrabi, S., Allemand, D. & Jaubert, J. 1993. Valine uptake by the scleractinian coral *Galaxea fascicularis:* characterization and effect of light and nutritional status. *J Comp Physiol B* **163**, 355–362. https://doi.org/10.1007/BF00265638

Altabet, M.A., 1988. Variations in nitrogen isotopic composition between sinking and suspended particles: implications for nitrogen cycling and particle transformation in the open ocean. Deep Sea Res. Part Oceanogr. Res. Pap. 35, 535–554. https://doi.org/10.1016/0198-0149(88)90130-6

Altabet, M.A., Deuser, W.G., Honjo, S., Stienen, C., 1991. Seasonal and depth-related changes in the source of sinking particles in the North Atlantic. Nature 354, 136–139. https://doi.org/10.1038/354136a0

Altabet, M.A., Francois, R., 1994. Sedimentary nitrogen isotopic ratio as a recorder for surface ocean nitrate utilization. Glob. Biogeochem. Cycles 8, 103–116. https://doi.org/10.1029/93GB03396

Altabet, M., Higginson, M. & Murray, D. 2002. The effect of millennial-scale changes in Arabian Sea denitrification on atmospheric CO_2. *Nature* **415**, 159–162. https://doi.org/10.1038/415159a

Ayliffe, L.K., Cerling, T.E., Robinson, T., West, A.G., Sponheimer, M., Passey, B.H., Hammer, J., Roeder, B., Dearing, M.D., Ehleringer, J.R., 2004. Turnover of carbon isotopes in tail hair and breath CO2 of horses fed an isotopically varied diet. Oecologia 139, 11–22. https://doi.org/10.1007/s00442-003-1479-x

Banas, N., Bricker, J., Carter, G., Gerdes, F., Martin, W., Nelson, E., Ross, T., Scansen, B., Simons, R., Wells, M., 1999. Flow, Stratification, and mixing in San Juan Channel.

Beauchamp, K.A., 1989. Aspects of gametogenesis, development and planulation in laboratory populations of solitary corals and corallimorpharian sea anemones (Ph.D.). University of California, Santa Cruz, United States -- California.

Böhlke, J.K., Mroczkowski, S.J., Coplen, T.B., 2003. Oxygen isotopes in nitrate: new reference materials for 18O:17O:16O measurements and observations on nitrate-water equilibration. Rapid Commun. Mass Spectrom. RCM 17, 1835–1846. https://doi.org/10.1002/rcm.1123

741 Braman, R.S., Hendrix, S.A., 1989. Nanogram nitrite and nitrate determination in environmental and biological
742 materials by vanadium(III) reduction with chemiluminescence detection. Anal. Chem. 61, 2715–2718.
743 https://doi.org/10.1021/ac00199a007

744 Brandes, J.A., Devol, A.H., 2002. A global marine-fixed nitrogen isotopic budget: Implications for Holocene
745 nitrogen cycling. Glob. Biogeochem. Cycles 16, 67-1-67–14. https://doi.org/10.1029/2001GB001856

746 Bronk, D. A. 2002. Dynamics of DON. Biogeochem. Mar. Dissolved Org. Matter 153–249.

747 Brown, B. E., & Bythell, J. C. 2005. Perspectives on mucus secretion in reef corals. *Marine Ecology Progress*
748 *Series*, *296*, 291–309. http://www.jstor.org/stable/24868640Cairns, S.D., 2007. Deep-water corals: an
749 overview with special reference to diversity and distribution of deep-water scleractinian corals. Bull.
750 Mar. Sci. 81, 311–322.

751 Carlier, A., Guilloux, E.L., Olu, K., Sarrazin, J., Mastrototaro, F., Taviani, M., Clavier, J., 2009. Trophic
752 relationships in a deep Mediterranean cold-water coral bank (Santa Maria di Leuca, Ionian Sea). Mar.
753 Ecol. Prog. Ser. 397, 125–137. https://doi.org/10.3354/meps08361

754 Carpenter, E. J., Harvey, H. R., Fry, B. & Capone, D. G. 1997. Biogeochemical tracers of the marine
755 cyanobacterium Trichodesmium. Deep-Sea Res. I 44, 27–38. doi.org/10.1016/S0967-0637(96)00091-X

756 Casciotti, K.L., Sigman, D.M., Hastings, M.G., Böhlke, J.K., Hilkert, A., 2002. Measurement of the oxygen
757 isotopic composition of nitrate in seawater and freshwater using the denitrifier method. Anal. Chem. 74,
758 4905–4912. https://doi.org/10.1021/ac020113w

759 Casciotti, K.L., Trull, T.W., Glover, D.M., Davies, D., 2008. Constraints on nitrogen cycling at the subtropical
760 North Pacific Station ALOHA from isotopic measurements of nitrate and particulate nitrogen. Deep Sea
761 Res. Part II Top. Stud. Oceanogr. 55, 1661–1672. https://doi.org/10.1016/j.dsr2.2008.04.017

762 Cathalot C, Van Oevelen D, Cox TJS, Kutti T., Lavaleye M., Duineveld G., Meysman F. J. R. 2015. Cold-water
763 coral reefs and adjacent sponge grounds: hotspots of benthic respiration and organic carbon cycling in the
764 deep sea. *Front Mar Sci* 2. https://www.frontiersin.org/articles/10.3389/fmars.2015.00037.

765 Cerling, T.E., Ayliffe, L.K., Dearing, M.D., Ehleringer, J.R., Passey, B.H., Podlesak, D.W., Torregrossa, A-M.,
766 West, A.G. 2007. Determining biological tissue turnover using stable isotopes: the reaction progress
767 variable. Ecophysiology 151, 175-189. https://doi.org/10.1007/s00442-006-0571-4

768 Chen, WH., Ren, H., Chiang, J.C.H. *et al.* Increased tropical South Pacific western boundary current transport
769 over the past century. *Nat. Geosci.* **16**, 590–596 (2023). https://doi.org/10.1038/s41561-023-01212-4

770 Cheng, H., Adkins, J., Edwards, R.L., Boyle, E.A., 2000. U-Th dating of deep-sea corals. Geochim. Cosmochim.
771 Acta 64, 2401–2416. https://doi.org/10.1016/S0016-7037(99)00422-6

772 Crook, E.D., Cooper, H., Potts, D.C., Lambert, T., Paytan, A., 2013. Impacts of food availability and pCO2 on
773 planulation, juvenile survival, and calcification of the azooxanthellate scleractinian coral Balanophyllia
774 elegans. Biogeosciences 10, 7599–7608. https://doi.org/10.5194/bg-10-7599-2013

775 Da Ros, Z., Dell'Anno, A., Fanelli, E., Angeletti, L., Taviani, M., Danovaro, R., 2022. Food preferences of
776 Mediterranean cold-water corals in captivity. Front. Mar. Sci. 9.

777 Del Bel Belluz, J., Peña, M.A., Jackson, J.M., Nemcek, N., 2021. Phytoplankton composition and environmental
778 drivers in the Northern Strait of Georgia (Salish Sea), British Columbia, Canada. Estuaries Coasts 44,
779 1419–1439. https://doi.org/10.1007/s12237-020-00858-2

780 De Pol-Holz R, Robinson RS, Hebbeln D, Sigman DM, Ulloa O. 2009. Controls on sedimentary nitrogen
781 isotopes along the Chile margin. *Deep Res Part II Top Stud Oceanogr* 56(16).
782 doi:10.1016/j.dsr2.2008.09.014

783 DiFiore, P.J., Sigman, D.M., Trull, T.W., Lourey, M.J., Karsh, K., Cane, G., Ho, R., 2006. Nitrogen isotope
784 constraints on subantarctic biogeochemistry. J. Geophys. Res. Oceans 111.
785 https://doi.org/10.1029/2005JC003216

786 Dodds, L.A., Black, K.D., Orr, H., Roberts, J.M., 2009. Lipid biomarkers reveal geographical differences in food
787 supply to the cold-water coral *Lophelia pertusa* (Scleractinia). Mar. Ecol. Prog. Ser. 397, 113–124.
788 https://doi.org/10.3354/meps08143

789 Doi, H., Akamatsu, F., González, A.L., 2017. Starvation effects on nitrogen and carbon stable isotopes of
790 animals: an insight from meta-analysis of fasting experiments. R. Soc. Open Sci. 4, 170633.
791 https://doi.org/10.1098/rsos.170633

792 Drake, J.L., Guillermic, M., Eagle, R.A., Jacobs, D.K., 2021. Fossil corals with various degrees of preservation
793 can retain information about biomineralization-related organic material. Front. Earth Sci. 9.

794 Druffel, E.R.M., 1997. Geochemistry of corals: Proxies of past ocean chemistry, ocean circulation, and climate.
795 Proc. Natl. Acad. Sci. 94, 8354–8361. https://doi.org/10.1073/pnas.94.16.8354

796 Duineveld, G.C.A., Lavaleye, M.S.S., Berghuis, E.M., 2004. Particle flux and food supply to a seamount cold-
797 water coral community (Galicia Bank, NW Spain). Mar. Ecol. Prog. Ser. 277, 13–23.
798 https://doi.org/10.3354/meps277013

799 Duineveld, G., Lavaleye, M., Bergman, M., Stigter, H., Mienis, F., 2007. Trophic structure of a cold-water coral
800 mound community (Rockall Bank, NE Atlantic) in relation to the near-bottom particle supply and current
801 regime. Bull. Mar. Sci. 81, 449–467.

802 Durham, J. W., and Barnard, J.L., 1952. Stony corals of the Eastern Pacific collected by the Velero III
803 and Velero IV. Al1an Hancock Pacific Expeditions 16, 1-110.

804 Erler, D.V., Wang, X.T., Sigman, D.M., Scheffers, S.R., Shepherd, B.O., 2015. Controls on the nitrogen isotopic
805 composition of shallow water corals across a tropical reef flat transect. Coral Reefs 34, 329–338.
806 https://doi.org/10.1007/s00338-014-1215-5

807 Esri. "Ocean" [basemap]. Scale Not Given. " Ocean Basemap ". February 11, 2021.
808 https://hub.arcgis.com/maps/CESPK::ocean-basemap/explore?location=35.956244%2C-
809 111.078800%2C5.00. (December, 2022).

810 Fadlallah, Y.H., 1983. Population Dynamics and Life History of a Solitary Coral, *Balanophyllia elegans*, from
811 Central California. Oecologia 58, 200–207.

812 Fautin, D.G., 2009. Structural diversity, systematics, and evolution of cnidae. Toxicon, Cnidarian Toxins and
813 Venoms 54, 1054–1064. https://doi.org/10.1016/j.toxicon.2009.02.024

814 Fawcett, S.E., Lomas, M.W., Casey, J.R., Ward, B.B., Sigman, D.M., 2011. Assimilation of upwelled nitrate by
815 small eukaryotes in the Sargasso Sea. Nat. Geosci. 4, 717–722. https://doi.org/10.1038/ngeo1265

816 Ferrier, M.D. 1991. Net uptake of dissolved free amino acids by four scleractinian corals. *Coral Reefs* **10**, 183–
817 187. https://doi.org/10.1007/BF00336772

François, R., Altabet, M.A., Yu, E.-F., Sigman, D.M., Bacon, M.P., Frank, M., Bohrmann, G., Bareille, G., Labeyrie, L.D., 1997. Contribution of Southern Ocean surface-water stratification to low atmospheric CO2 concentrations during the last glacial period. Nature 389, 929–935. https://doi.org/10.1038/40073

Freiwald, A. 2002. Reef-Forming Cold-Water Corals. In: Wefer, G., Billett, D., Hebbeln, D., Jørgensen, B.B., Schlüter, M., van Weering, T.C.E. (eds) Ocean Margin Systems. Springer, Berlin, Heidelberg. https://doi.org/10.1007/978-3-662-05127-6_23

Gagnon, A.C., Gothmann, A.M., Branson, O., Rae, J.W.B., Stewart, J.A., 2021. Controls on boron isotopes in a cold-water coral and the cost of resilience to ocean acidification. Earth and Planetary Science Letters 554, 116662. https://doi.org/10.1016/j.epsl.2020.116662

Ganeshram, R. S., and Pedersen, T. F. 1998, Glacial-interglacial variability in upwelling and bioproductivity off NW Mexico: Implications for Quaternary paleoclimate, *Paleoceanography*, 13(6), 634– 645, doi:10.1029/98PA02508.

Garcia-Herrera, N., Cornils, A., Laudien, J., Niehoff, B., Höfer, J., Försterra, G., González, H.E., Richter, C., 2022. Seasonal and diel variations in the vertical distribution, composition, abundance and biomass of zooplankton in a deep Chilean Patagonian Fjord. PeerJ 10, e12823. https://doi.org/10.7717/peerj.12823

Genin, A., Dayton, P.K., Lonsdale, P.F., Spiess, F.N., 1986. Corals on seamount peaks provide evidence of current acceleration over deep-sea topography. Nature 322, 59–61. https://doi.org/10.1038/322059a0

Gerrodette, T. 1981. Equatorial Submergence in a Solitary Coral, Balanophyllia elegans, and the Critical Life Stage Excluding the Species from Shallow Water in the South. Mar. Ecol. Prog. Series 1, 227-235. http://www.jstor.org/stable/24812947.

Gonfiantini, R., W. Stichler, and K. Rosanski 1995, Standards and Intercomparison. Materials Distributed by the IAEA for Stable Isotope Measurements,Int. At. Energy Agency, Vienna.

Goodfriend, G.A., Hare, P.E., Druffel, E.R.M. 1992. Aspartic acid racemization and protein diagenesis in corals over the last 350 years. Geochim. Cosmochim. Acta 56, 3847–3850. https://doi.org/10.1016/0016-7037(92)90176-J

Gori, A., R. Grover, C. Orejas, S. Sikorski, and C. Ferrier-Pagès. 2014. Uptake of dissolved free amino acids by four cold-water coral species from the Mediterranean Sea. Deep Sea Res. Part II Top. Stud. Oceanogr. **99**: 42–50. doi:10.1016/j.dsr2.2013.06.007

Gothmann AM, Stolarski J, Adkins JF, et al. Fossil corals as an archive of secular variations in seawater chemistry since the Mesozoic. *Geochim Cosmochim Acta*. 2015;160:188-208. doi:https://doi.org/10.1016/j.gca.2015.03.018

Grover, R. Maguer, J-F, Allemand, D., Ferrier-Pagès, C. 2008. Uptake of dissolved free amino acids by the scleractinian coral *Stylophora pistillata*. *J Exp Biol* 211 (6): 860–865. doi: https://doi.org/10.1242/jeb.012807

Hannides, Cecelia C. S., Popp, Brian N., Choy, C. Anela, Drazen, Jeffrey C. 2013. Midwater zooplankton and suspended particle dynamics in the North Pacific Subtropical Gyre: A stable isotope perspective, *Limnology and Oceanography*, 58, doi: 10.4319/lo.2013.58.6.1931.

Hill, T.M., Myrvold, C.R., Spero, H.J., Guilderson, T.P. 2014. Evidence for benthic and pelagic food web coupling and carbon export from California margin bamboo coral archives. *Biogeosciences* 11, 3845–3854. https://doi.org/10.5194/bg-11-3845-2014

Hines, S.K.V., Southon, J.R., Adkins, J.F. 2015. A high-resolution record of Southern Ocean intermediate water radiocarbon over the past 30,000 years. *Earth and Planetary Science Letters* 432, 46-58. https://doi.org/10.1016/j.epsl.2015.09.038

Hoegh-Guldberg, O., Williamson, J. Availability of two forms of dissolved nitrogen to the coral Pocillopora damicornis and its symbiotic zooxanthellae. *Marine Biology* **133**, 561–570 (1999). https://doi.org/10.1007/s002270050496

Höfer, J., González, H.E., Laudien, J., Schmidt, G.M., Häussermann, V., Richter, C., 2018. All you can eat: the functional response of the cold-water coral *Desmophyllum dianthus* feeding on krill and copepods. PeerJ 6, e5872. https://doi.org/10.7717/peerj.5872

Horn, M.G., Robinson, R.S., Rynearson, T.A., Sigman, D.M., 2011. Nitrogen isotopic relationship between diatom-bound and bulk organic matter of cultured polar diatoms. Paleoceanography 26. https://doi.org/10.1029/2010PA002080

Kast, E.R., Stolper, D.A., Auderset, A., Higgins, J.A., Ren, H., Wang, X.T., Martínez-García, A., Haug, G.H., Sigman, D.M., 2019. Nitrogen isotope evidence for expanded ocean suboxia in the early Cenozoic. Science 364, 386–389. https://doi.org/10.1126/science.aau5784

Kiriakoulakis, K., Fisher, E., Wolff, G.A., Freiwald, A., Grehan, A., Roberts, J.M., 2005. Lipids and nitrogen isotopes of two deep-water corals from the North-East Atlantic: initial results and implications for their nutrition, in: Freiwald, A., Roberts, J.M. (Eds.), Cold-Water Corals and Ecosystems, Erlangen Earth Conference Series. Springer, Berlin, Heidelberg, pp. 715–729. https://doi.org/10.1007/3-540-27673-4_37

Knapp, A. N., K. L. Casciotti, and M. G. Prokopenko. 2018. Dissolved Organic Nitrogen Production and Consumption in Eastern Tropical South Pacific Surface Waters. Glob. Biogeochem. Cycles **32**: 769–783. doi:10.1029/2017GB005875

Knapp AN, DiFiore PJ, Deutsch C, Sigman DM, Lipschultz F. 2008. Nitrate isotopic composition between Bermuda and Puerto Rico: Implications for N2 fixation in the Atlantic Ocean. *Global Biogeochem Cycles* 22(3). doi:10.1029/2007GB003107

Koppelmann, R., Böttger-Schnack, R., Möbius, J., Weikert, H., 2009. Trophic relationships of zooplankton in the eastern Mediterranean based on stable isotope measurements. Journal of Plankton Research 31, 669-686.

Lasker, H.R., 1981. A comparison of the particulate feeding abilities of three species of Gorgonian soft coral. Mar. Ecol. Prog. Ser. 5, 61–67.

Lewis, A.G., 1978. Concentrations of nutrients and chlorophyll on a cross-channel transect in Juan de Fuca Strait, British Columbia. J. Fish. Res. Board Can. 35, 305–314. https://doi.org/10.1139/f78-055

Lewis, J.B., Price, W.S., 1975. Feeding mechanisms and feeding strategies of Atlantic reef corals. J. Zool. 176, 527–544. https://doi.org/10.1111/j.1469-7998.1975.tb03219.x

Li, T., Robinson, L.F., Chen, T., Wang, X.T., Burke, A., Rae, J.W.B., Pegrum-Haram, A., Knowles, T.D.J., Li, G., Chen, J., Ng, H.C., Prokopenko, M., Rowland, G.H., Samperiz, A., Stewart, J.A., Southon, J., Spooner, P.T., 2020. Rapid shifts in circulation and biogeochemistry of the Southern Ocean during deglacial carbon cycle events. Science Advances 6, eabb3807

Lourey, M.J., Trull, T.W., Sigman, D.M., 2003. Sensitivity of δ15N of nitrate, surface suspended and deep sinking particulate nitrogen to seasonal nitrate depletion in the Southern Ocean. Glob. Biogeochem. Cycles 17. https://doi.org/10.1029/2002GB001973

Mackas, D.L., Harrison, P.J., 1997. Nitrogenous nutrient sources and sinks in the Juan de Fuca Strait/Strait of Georgia/Puget Sound estuarine system: Assessing the potential for eutrophication. Estuar. Coast. Shelf Sci. 44, 1–21. https://doi.org/10.1006/ecss.1996.0110

Maier, S.R., Bannister, R.J., van Oevelen, D., Kutti, T., 2020. Seasonal controls on the diet, metabolic activity, tissue reserves and growth of the cold-water coral *Lophelia pertusa*. Coral Reefs 39, 173–187. https://doi.org/10.1007/s00338-019-01886-6

Maier, S.R., Kutti, T., Bannister, R.J., van Breugel, P., van Rijswijk, P., van Oevelen, D., 2019. Survival under conditions of variable food availability: Resource utilization and storage in the cold-water coral *Lophelia pertusa*. Limnol. Oceanogr. 64, 1651–1671. https://doi.org/10.1002/lno.11142

Maier, S.R., Brooke, S., De Clippele, L.H., de Froe, E., van der Kaaden, A.-S., Kutti, T., Mienis, F., van Oevelen, D., 2023. On the paradox of thriving cold-water coral reefs in the food-limited deep sea. Biological Reviews 98, 1768–1795. https://doi.org/10.1111/brv.12976

Marconi D, Weigand AM, Rafter PA, Matthew R. McIlvin MR, Matthew Forbes, M Casciotti, KL Sigman, DM. 2015. Nitrate isotope distributions on the US GEOTRACES North Atlantic cross-basin section: Signals of polar nitrate sources and low latitude nitrogen cycling. *Mar Chem*. 177:143-156. doi:https://doi.org/10.1016/j.marchem.2015.06.007

Margolin, A. R., L. F. Robinson, A. Burke, R. G. Waller, K. M. Scanlon, M. L. Roberts, M. E. Auro, and T. van de Flierdt. 2014. Temporal and spatial distributions of cold-water corals in the Drake Passage: Insights from the last 35,000 years. Deep Sea Res. Part II Top. Stud. Oceanogr. **99**: 237–248. doi:10.1016/j.dsr2.2013.06.008

Mariotti, A., Germon, J.C., Hubert, P., Kaiser, P., Letolle, R., Tardieux, A., Tardieux, P., 1981. Experimental determination of nitrogen kinetic isotope fractionation: Some principles; illustration for the denitrification and nitrification processes. Plant Soil 62, 413–430. https://doi.org/10.1007/BF02374138

Martínez del Rio, C., Carleton, S.A., 2012. How fast and how faithful: the dynamics of isotopic incorporation into animal tissues. J. Mammal. 93, 353–359. https://doi.org/10.1644/11-MAMM-S-165.1

McCutchan Jr, J.H., Lewis Jr, W.M., Kendall, C., McGrath, C.C., 2003. Variation in trophic shift for stable isotope ratios of carbon, nitrogen, and sulfur. Oikos 102, 378–390. https://doi.org/10.1034/j.1600-0706.2003.12098.x

McIlvin, M.R., Casciotti, K.L., 2011. Technical Updates to the Bacterial Method for Nitrate Isotopic Analyses. Anal. Chem. 83, 1850–1856. https://doi.org/10.1021/ac1028984

McMahon, K.W., Williams, B., Guilderson, T.P., Glynn, D.S., McCarthy, M.D., 2018. Calibrating amino acid δ13C and δ15N offsets between polyp and protein skeleton to develop proteinaceous deep-sea corals as paleoceanographic archives. Geochim. Cosmochim. Acta 220, 261–275. https://doi.org/10.1016/j.gca.2017.09.048

Middelburg, J., Mueller, C., Veuger, B. Larsson, A. I., Form, A., van Oevelen, D 2016.. Discovery of symbiotic nitrogen fixation and chemoautotrophy in cold-water corals. *Sci Rep* **5**, 17962 (2016). https://doi.org/10.1038/srep17962

Miller, M., 1995. Growth of a temperate coral: effects of temperature, light, depth, and heterotrophy. Mar. Ecol. Prog. Ser. 122, 217–225. https://doi.org/10.3354/meps122217

Minagawa, M., Wada, E., 1984. Stepwise enrichment of 15N along food chains: Further evidence and the relation between δ15N and animal age. Geochim. Cosmochim. Acta 48, 1135–1140. https://doi.org/10.1016/0016-7037(84)90204-7

Mortensen P.B., (2001) Aquarium observations on the deep-water coral *Lophelia pertusa* (L., 1758) (scleractinia) and selected associated invertebrates, Ophelia, 54:2, 83-104, DOI: 10.1080/00785236.2001.10409457

Muhs, D.R., Kennedy, G.L., Rockwell, T.K., 1994. Uranium-Series Ages of Marine Terrace Corals from the Pacific Coast of North America and Implications for Last-Interglacial Sea Level History. Quaternary Research 42, 72–87. https://doi.org/10.1006/qres.1994.1055

Mueller, C.E., Larsson, A.I., Veuger, B., Middelburg, J.J., van Oevelen, D., 2014. Opportunistic feeding on various organic food sources by the cold-water coral *Lophelia pertusa*. Biogeosciences 11, 123–133. https://doi.org/10.5194/bg-11-123-2014

Murray, J.W., Roberts, E., Howard, E., O'Donnell, M., Bantam, C., Carrington, E., Foy, M., Paul, B., Fay, A., 2015. An inland sea high nitrate-low chlorophyll (HNLC) region with naturally high pCO2. Limnol. Oceanogr. 60, 957–966. https://doi.org/10.1002/lno.10062

Muscatine, L., Goiran, C., Land, L., Jaubert, J., Cuif, J.-P., Allemand, D., 2005. Stable isotopes (δ13C and δ15N) of organic matrix from coral skeleton. Proc. Natl. Acad. Sci. 102, 1525–1530. https://doi.org/10.1073/pnas.0408921102

Naumann, M.S., Orejas, C., Wild, C., Ferrier-Pagès, C., 2011. First evidence for zooplankton feeding sustaining key physiological processes in a scleractinian cold-water coral. J. Exp. Biol. 214, 3570–3576. https://doi.org/10.1242/jeb.061390

Naumann, M.S., Tolosa, I., Taviani, M., Grover, R., Ferrier-Pagès, C., 2015. Trophic ecology of two cold-water coral species from the Mediterranean Sea revealed by lipid biomarkers and compound-specific isotope analyses. Coral Reefs 34, 1165–1175. https://doi.org/10.1007/s00338-015-1325-8

Pride C, Thunell R, Sigman D, Keigwin L, Altabet M, Tappa E. 1999. Nitrogen isotopic variations in the Gulf of California since the Last Deglaciation: Response to global climate change. *Paleoceanography* 14(3). doi:10.1029/1999PA900004

967 Purser A, Larsson AI, Thomsen L, van Oevelen D. 2010. The influence of flow velocity and food concentration
968 on *Lophelia pertusa* (Scleractinia) zooplankton capture rates. *J Exp Mar Bio Ecol*. 395(1):55-62.
969 doi:https://doi.org/10.1016/j.jembe.2010.08.013

970 Rae, J.W.B. 2018. Boron Isotopes in Foraminifera: Systematics, Biomineralisation, and CO_2 Reconstruction. In:
971 Marschall, H., Foster, G. (eds) Boron Isotopes. Advances in Isotope Geochemistry. Springer, Cham.
972 https://doi.org/10.1007/978-3-319-64666-4_5

973 Rangel, M.S., Erler, D., Tagliafico, A., Cowden, K., Scheffers, S., Christidis, L., 2019. Quantifying the transfer
974 of prey δ15N signatures into coral holobiont nitrogen pools. Mar. Ecol. Prog. Ser. 610, 33–49.
975 https://doi.org/10.3354/meps12847

976 Ren, H., Sigman, D.M., Meckler, A.N., Plessen, B., Robinson, R.S., Rosenthal, Y., Haug, G.H., 2009.
977 Foraminiferal Isotope Evidence of Reduced Nitrogen Fixation in the Ice Age Atlantic Ocean. Science
978 323, 244–248. https://doi.org/10.1126/science.1165787

979 Reynaud, S., Martinez, P., Houlbrèque, F., Billy, I., Allemand, D., Ferrier-Pagès, C., 2009. Effect of light and
980 feeding on the nitrogen isotopic composition of a zooxanthellate coral: role of nitrogen recycling. Mar.
981 Ecol. Prog. Ser. 392, 103–110. https://doi.org/10.3354/meps08195

982 Roberts, J.M., Wheeler, A.J., Freiwald, A., 2006. Reefs of the deep: The biology and geology of cold-water coral
983 ecosystems. Science 312, 543–547. https://doi.org/10.1126/science.1119861

984 Robinson, R.S., Kienast, M., Albuquerque, A.L., Altabet, M., Contreras, S., Holz, R.D.P., Dubois, N., Francois,
985 R., Galbraith, E., Hsu, T.-C., Ivanochko, T., Jaccard, S., Kao, S.-J., Kiefer, T., Kienast, S., Lehmann, M.,
986 Martinez, P., McCarthy, M., Möbius, J., Pedersen, T., Quan, T.M., Ryabenko, E., Schmittner, A.,
987 Schneider, R., Schneider-Mor, A., Shigemitsu, M., Sinclair, D., Somes, C., Studer, A., Thunell, R., Yang,
988 J.-Y., 2012. A review of nitrogen isotopic alteration in marine sediments. Paleoceanography 27.
989 https://doi.org/10.1029/2012PA002321

990 Robinson LF, Adkins JF, Frank N, Gagnon, A.C., Prouty, N.G., Roark, B. van de Flierdt, T. 2014. The
991 geochemistry of deep-sea coral skeletons: A review of vital effects and applications for
992 palaeoceanography. *Deep Sea Res Part II Top Stud Oceanogr*. 99:184-198.
993 doi:https://doi.org/10.1016/j.dsr2.2013.06.005

994 Robinson RS, Sigman DM. 2008. Nitrogen isotopic evidence for a poleward decrease in surface nitrate within the
995 ice age Antarctic. *Quat Sci Rev*. 27(9-10). doi:10.1016/j.quascirev.2008.02.005

996 Robinson, R.S., Smart, S.M., Cybulski, J.D., McMahon, K.W., Marcks, B., Nowakowski, C., 2023. Insights from
997 fossil-bound nitrogen isotopes in diatoms, foraminifera, and corals. Annu. Rev. Mar. Sci. 15, null.
998 https://doi.org/10.1146/annurev-marine-032122-104001

999 Ryan, W. B. F., S.M. Carbotte, J. Coplan, S. O'Hara, A. Melkonian, R. Arko, R.A. Weissel, V. Ferrini, A.
1000 Goodwillie, F. Nitsche, J. Bonczkowski, R. Zemsky, 2009. Global Multi-Resolution Topography
1001 (GMRT) synthesis data set, *Geochem. Geophys. Geosyst.*, 10, Q03014, doi:10.1029/2008GC002332.

1002 Saino, T., Hattori, A., 1987. Geographical variation of the water column distribution of suspended particulate
1003 organic nitrogen and its 15N natural abundance in the Pacific and its marginal seas. Deep Sea Res. A 34,
1004 807–827. https://doi.org/10.1016/0198-0149(87)90038-0

Scrimgeour, C.M., Gordon, S.C., Handley, L.L., Woodford, J.A.T., 1995. Trophic levels and anomalous δ15N of insects on raspberry (Rubus Idaeus L.). Isotopes Environ. Health Stud. 31, 107–115. https://doi.org/10.1080/10256019508036256

Sebens, K.P., Vandersall, K.S., Savina, L.A., Graham, K.R., 1996. Zooplankton capture by two scleractinian corals, Madracis mirabilis andMontastrea cavernosa, in a field enclosure. Mar. Biol. 127, 303–317. https://doi.org/10.1007/BF00942116

Sherwood, O.A., Heikoop, J.M., Scott, D.B., Risk, M.J., Guilderson, T.P., McKinney, R.A., 2005. Stable isotopic composition of deep-sea gorgonian corals *Primnoa* spp.: a new archive of surface processes. Mar. Ecol. Prog. Ser. 301, 135–148. https://doi.org/10.3354/meps301135

Sherwood, O.A., Jamieson, R.E., Edinger, E.N., Wareham, V.E., 2008. Stable C and N isotopic composition of cold-water corals from the Newfoundland and Labrador continental slope: Examination of trophic, depth and spatial effects. Deep Sea Res. Part Oceanogr. Res. Pap. 55, 1392–1402. https://doi.org/10.1016/j.dsr.2008.05.013

Sherwood, O.A., Thresher, R.E., Fallon, S.J., Davies, D.M., Trull, T.W., 2009. Multi-century time-series of ^{15}N and ^{14}C in bamboo corals from deep Tasmanian seamounts: evidence for stable oceanographic conditions. Mar. Ecol. Prog. Ser. 397, 209–218. https://doi.org/10.3354/meps08166

Sigman, D.M., Altabet, M.A., McCorkle, D.C., Francois, R., Fischer, G., 1999. The $\delta^{15}N$ of nitrate in the Southern Ocean: Consumption of nitrate in surface waters. Glob. Biogeochem. Cycles 13, 1149–1166. https://doi.org/10.1029/1999GB900038

Sigman, D., Boyle, E. Glacial/interglacial variations in atmospheric carbon dioxide. 2000. *Nature* **407**, 859–869 (2000). https://doi.org/10.1038/35038000

Sigman, D.M., Casciotti, K.L., Andreani, M., Barford, C., Galanter, M., Böhlke, J.K., 2001. A Bacterial method for the nitrogen isotopic analysis of nitrate in seawater and freshwater. Anal. Chem. 73, 4145–4153. https://doi.org/10.1021/ac010088e

Sigman, D.M., Fripiat, F., 2019. *Nitrogen Isotopes in the Ocean*, in: Cochran, J.K., Bokuniewicz, H.J., Yager, P.L. (Eds.), Encyclopedia of Ocean Sciences (Third Edition). Academic Press, Oxford, pp. 263–278. https://doi.org/10.1016/B978-0-12-409548-9.11605-7

Soetaert, K., Mohn, C., Rengstorf, A., Grehan, A., van Oevelen, D., 2016. Ecosystem engineering creates a direct nutritional link between 600-m deep cold-water coral mounds and surface productivity. Sci. Rep. 6, 35057. https://doi.org/10.1038/srep35057

Spero, H.J., Andreasen, D.J., Sorgeloos, P., 1993. Carbon and nitrogen isotopic composition of different strains of *Artemia* sp. Int. J. Salt Lake Res. 2, 133. https://doi.org/10.1007/BF02905905

Studer, A.S., Sigman, D.M., Martinez-Garcia, A., Thole, L.M., Michel, E., Jaccard, S.L., Lippolds, J.A., Mazaud, A., Wang, X.C.T., Robinson, L.F., Adkins, J.F., Haug, G.H., 2018. Increased nutrient supply to the Southern Ocean during the Holocene and its implications for the pre-industrial atmospheric CO2 rise. Nat Geosci 11, 756-761

Tanaka, Y., Miyajima, T., Koike, I., Hayashibara, T., Ogawa, H., 2006. Translocation and conservation of organic nitrogen within the coral-zooxanthella symbiotic system of Acropora pulchra, as demonstrated

by dual isotope-labeling techniques. J. Exp. Mar. Biol. Ecol. 336, 110–119. https://doi.org/10.1016/j.jembe.2006.04.011

Tanaka, Y., Suzuki, A., Sakai, K., 2018. The stoichiometry of coral-dinoflagellate symbiosis: carbon and nitrogen cycles are balanced in the recycling and double translocation system. ISME J. 12, 860–868. https://doi.org/10.1038/s41396-017-0019-3

Teece, M.A., Estes, B., Gelsleichter, E., Lirman, D., 2011. Heterotrophic and autotrophic assimilation of fatty acids by two scleractinian corals, Montastraea faveolata and Porites astreoides. Limnol. Oceanogr. 56, 1285–1296. https://doi.org/10.4319/lo.2011.56.4.1285

Thiagarajan N., Subhas A. V., Southon J. R., Eiler J. M. andAdkins J. F. 2014. Abrupt pre-Bolling-Allerod warming and circulation changes in the deep ocean. Nature 511, 75–78. https://doi.org/10.1038/nature13472

Thiem, Ø., Ravagnan, E., Fosså, J.H., Berntsen, J., 2006. Food supply mechanisms for cold-water corals along a continental shelf edge. J. Mar. Syst. 60, 207–219. https://doi.org/10.1016/j.jmarsys.2005.12.004

Thomas, S.M., Crowther, T.W., 2015. Predicting rates of isotopic turnover across the animal kingdom: a synthesis of existing data. J. Anim. Ecol. 84, 861–870. https://doi.org/10.1111/1365-2656.12326

Treibergs, L.A., Fawcett, S.E., Lomas, M.W., Sigman, D.M., 2014. Nitrogen isotopic response of prokaryotic and eukaryotic phytoplankton to nitrate availability in Sargasso Sea surface waters. Limnol. Oceanogr. 59, 972–985. https://doi.org/10.4319/lo.2014.59.3.0972

Tsounis G, Orejas C, Reynaud S, JM G, Allemand D, Ferrier-Pagès C. 2010. Prey-capture rates in four Mediterranean cold water corals . *Mar Ecol Prog Ser*. 398:149-155. https://doi.org/10.3354/meps08312

van Oevelen, P., Duineveld, G., Lavaleye, M., Mienis, Furu, Soetaert, Karline, H., Carlo H. R., 2009. The cold-water coral community as hotspot of carbon cycling on continental margins: A food-web analysis from Rockall Bank (northeast Atlantic), *Limnology and Oceanography*, 54, doi: 10.4319/lo.2009.54.6.1829.

Vinogradov, M. E. Feeding of the deep-sea zooplankton. 1962. *Rapp. Pv. Reun. Cons. Perm. Int. Exp. Mer.* **153**, 114–120.

Wang, X.T., Prokopenko, M.G., Sigman, D.M., Adkins, J.F., Robinson, L.F., Ren, H., Oleynik, S., Williams, B., Haug, G.H., 2014. Isotopic composition of carbonate-bound organic nitrogen in deep-sea scleractinian corals: A new window into past biogeochemical change. Earth Planet. Sci. Lett. 400, 243–250. https://doi.org/10.1016/j.epsl.2014.05.048

Wang, X.T., Sigman, D.M., Prokopenko, M.G., Adkins, J.F., Robinson, L.F., Hines, S.K., Chai, J., Studer, A.S., Martínez-García, A., Chen, T., Haug, G.H., 2017. Deep-sea coral evidence for lower Southern Ocean surface nitrate concentrations during the last ice age. Proc. Natl. Acad. Sci. 114, 3352–3357. https://doi.org/10.1073/pnas.1615718114

Webb, S., Hedges, R., Simpson, S., 1998. Diet quality influences the $\delta^{13}C$ and $\delta^{15}N$ of locusts and their biochemical components. J. Exp. Biol. 201, 2903–2911. https://doi.org/10.1242/jeb.201.20.2903

Weigand, M.A., Foriel, J., Barnett, B., Oleynik, S., Sigman, D.M., 2016. Updates to instrumentation and protocols for isotopic analysis of nitrate by the denitrifier method. Rapid Commun. Mass Spectrom. 30, 1365–1383. https://doi.org/10.1002/rcm.7570

1081 Williams, B., and Grottoli, A. G. 2010. Recent shoaling of the nutricline and thermocline in the western tropical
1082 Pacific, *Geophys. Res. Lett.*, 37, L22601, doi:10.1029/2010GL044867.

1083 Zhang, R., X. T. Wang, H. Ren, J. Huang, M. Chen, and D. M. Sigman. 2020. Dissolved Organic Nitrogen
1084 Cycling in the South China Sea From an Isotopic Perspective. Glob. Biogeochem. Cycles **34**:
1085 e2020GB006551. doi:10.1029/2020GB006551

1086 Zhou, M., Granger, J., Chang, B.X., 2022. Influence of sample volume on nitrate N and O isotope ratio analyses
1087 with the denitrifier method. Rapid Commun. Mass Spectrom. 36, e9224.
1088 https://doi.org/10.1002/rcm.9224